



**HAL**  
open science

## A Benchmark Database for Mixed-Solvent Electrolyte Solutions: Consistency Analysis using E-NRTL

Fufang Yang, Tri Dat Ngo, Georgios Kontogeorgis, Jean-Charles de Hemptinne

► **To cite this version:**

Fufang Yang, Tri Dat Ngo, Georgios Kontogeorgis, Jean-Charles de Hemptinne. A Benchmark Database for Mixed-Solvent Electrolyte Solutions: Consistency Analysis using E-NRTL. *Industrial and engineering chemistry research*, 2022, 61 (42), pp.15576-15593. 10.1021/acs.iecr.2c00059 . hal-03941779

**HAL Id: hal-03941779**

**<https://ifp.hal.science/hal-03941779>**

Submitted on 16 Jan 2023

**HAL** is a multi-disciplinary open access archive for the deposit and dissemination of scientific research documents, whether they are published or not. The documents may come from teaching and research institutions in France or abroad, or from public or private research centers.

L'archive ouverte pluridisciplinaire **HAL**, est destinée au dépôt et à la diffusion de documents scientifiques de niveau recherche, publiés ou non, émanant des établissements d'enseignement et de recherche français ou étrangers, des laboratoires publics ou privés.

# 1 **A benchmark database for mixed-solvent electrolyte solutions:** 2 **Consistency analysis using E-NRTL**

3 Fufang Yang <sup>1,2</sup>, Tri Dat Ngo <sup>1</sup>, Georgios M. Kontogeorgis <sup>2</sup>, Jean-Charles de Hemptinne <sup>1\*</sup>

4 <sup>1</sup> IFP Energies Nouvelles, 1 et 4 Avenue de Bois-Préau, 92852 Rueil-Malmaison Cedex, France

5 <sup>2</sup> Center for Energy Resources Engineering (CERE), Department of Chemical and Biochemical  
6 Engineering, Technical University of Denmark, 2800 Kgs. Lyngby, Denmark

7 \* Corresponding author: jean-charles.de-hemptinne@ifpen.fr

8 **Abstract:** Modeling of thermodynamic properties of mixed-solvent electrolyte solutions is  
9 challenging. Reliable experimental data are essential for any model development and  
10 parameterization. In this work, a benchmark database for (water + methanol/ethanol + alkali halide)  
11 mixed-solvent electrolyte solutions is presented. Available experimental data of mean ionic activity  
12 coefficient (MIAC) and vapor-liquid equilibrium (VLE) are comprehensively collected and  
13 critically evaluated for 61 datasets of 23 solutions. The resulting benchmark database includes 1413  
14 data records from 32 datasets for 13 solutions. Evaluated datasets of the relevant aqueous  
15 electrolyte solutions are also presented. A consistent E-NRTL model that satisfies the Gibbs-  
16 Duhem equation is utilized for analyzing the data, reconciling the MIAC and VLE data. The  
17 collected data are critically evaluated. A benchmark database is obtained. Based on the database,  
18 recommended parameters are obtained for the E-NRTL model.

19 **Keywords:** benchmark database, consistent E-NRTL, mixed-solvent electrolyte solution, mean  
20 ionic activity coefficient, vapor-liquid equilibrium

## 21 **1 Introduction**

22 Electrolyte solutions are important in many industrial processes, e.g., CO<sub>2</sub> capture and  
23 sequestration <sup>1</sup>, flue gas treatment <sup>2</sup>, desalination <sup>3</sup>, scale formation <sup>4</sup>, corrosion resistance  
24 enhancement <sup>5</sup>, batteries <sup>6</sup>, pharmaceutical processes <sup>7</sup>, etc. Reliable experimental data are essential  
25 for thermodynamic property model development and process system modeling, while incomplete

26 and inaccurate data hampers their utilization <sup>8</sup>. Because of the complexity of the interactions that  
27 take place in electrolyte solutions, the existing thermodynamic models are not well adapted to those  
28 mixtures <sup>9</sup>; available tools are not yet well accepted and validated as for non-electrolyte systems <sup>10</sup>;  
29 the physics of the competing contributions is not yet well understood <sup>11,12</sup>. Furthermore, over the  
30 past century, experimental data have been reported in dozens of conventions <sup>13</sup>, e.g., different  
31 reference states and composition units. In addition, for mixed-solvent electrolyte solutions,  
32 experimental data from different sources are frequently not consistent with each other. Thus,  
33 obtaining a reliable database needs comprehensive collection and critical evaluation of available  
34 experimental data.

35 In a previous work <sup>14</sup>, a benchmark database is proposed for aqueous alkali halide solutions.  
36 For mixed-solvent electrolyte solutions, the extra solvent brings in an extra dimension in  
37 composition, complexing property comparisons. Furthermore, the solvation and dissociation  
38 behavior of electrolytes is very different in water and non-water solvents. Various equations of  
39 state <sup>15-25</sup> and activity coefficient models <sup>26-38</sup> have been applied on these mixtures. Because of the  
40 complexity from both experimental and theoretical perspectives, a benchmark database for  
41 important mixtures of the type can facilitate future model development, parameterization, and  
42 evaluation. In addition, compared to the data status of aqueous electrolyte solutions, that of mixed-  
43 solvent electrolyte solutions is much scarcer. Therefore, data analysis requires a model that applies  
44 on mixed-solvent electrolyte systems and does not include too many adjustable parameters.

45 Although modern thermodynamic models are of theoretical basis. As parameters are regressed,  
46 accurate correlation of the experimental data does not guarantee data reliability. Therefore, critical  
47 evaluation of the experimental data needs comparisons between data from different sources and of  
48 different properties, as well as comparisons within a series of salts in the same solvents. To achieve  
49 this, a consistent version of the E-NRTL model is introduced, satisfying the Gibbs-Duhem equation,  
50 and thus facilitating verification between the mean ionic activity coefficient (MIAC) and vapor-  
51 liquid equilibrium (VLE), which includes information of the ionic and solvent activity coefficients,  
52 respectively. The consistent model is similar to the consistent model proposed by van Bochove et  
53 al. <sup>31</sup>, short of the Bronsted-Guggenheim term <sup>39,40</sup>.

54 Our aim is to present a benchmark database based on an extensive evaluation of available  
55 experimental data, to recommend parameters based on this database, and to understand trends of

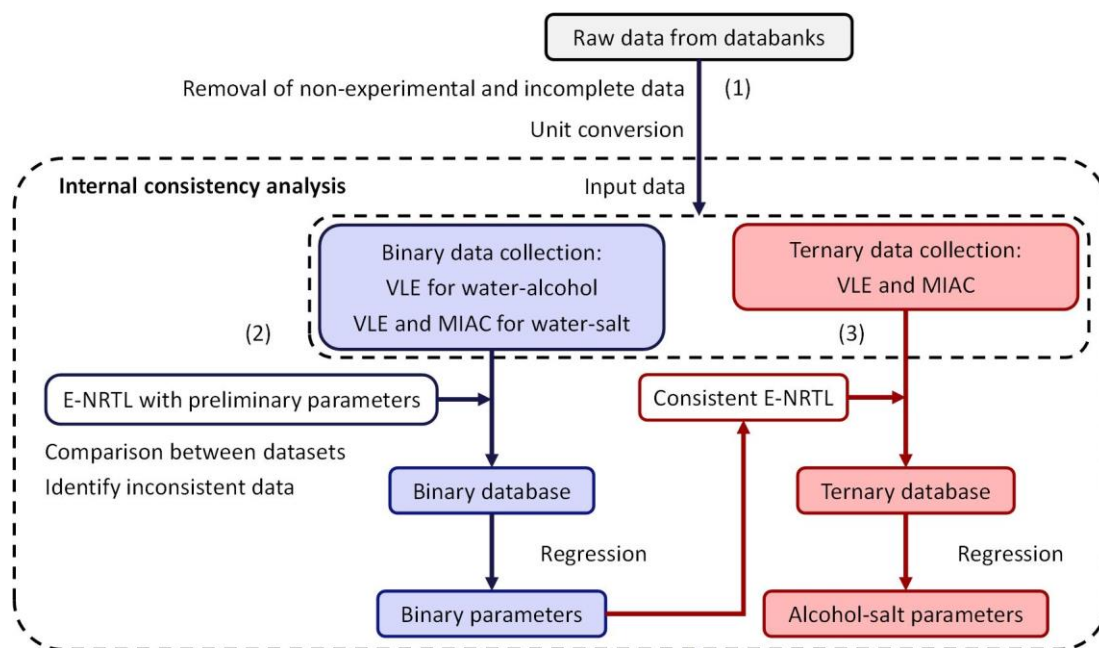
56 data and parameters. The work proceeds as follows. First, the overall data analysis framework is  
57 introduced. Then, the consistent E-NRTL model is introduced and compared with the widely used  
58 original E-NRTL. Then, a consistency analysis is performed for each mixture. Impacts of the  
59 objective function and water-salt parameters on the representation of mixed-solvent electrolyte  
60 solution properties are investigated, concluding on a parameter regression procedure that facilitates  
61 the data analysis framework. Based on these findings, the alcohol-salt parameters and ternary  
62 property results are presented. Finally, the obtained benchmark database of the mixed-solvent  
63 electrolyte systems and the involved aqueous electrolyte systems is proposed.

## 64 **2 Data analysis framework**

65 This section introduces the properties' definitions and relationships with the activity  
66 coefficients, the composition denotations, and the raw data collected from the databanks. Figure 1  
67 shows the data analysis framework. The following path is followed:

- 68 (1) We start from the raw data collected from the databanks. Datasets that are non-experimental  
69 and incomplete (e.g., datasets that are not in tabular forms, and VLE datasets without vapor  
70 phase molar fraction) are removed. The experimental datasets were reported in many different  
71 composition units. They are converted to ion-based molar fraction, i.e., full dissociation is  
72 assumed, and the cation and anion are considered as two species. For the (water + alcohol)  
73 mixtures, VLE data are collected. For the (water + salt) and (water + alcohol + salt) mixtures,  
74 VLE and MIAC data are collected. For mixtures containing two solvents, only the VLE  
75 datasets that include both vapor pressure and vapor phase molar fraction data are collected,  
76 because solvent activity coefficient requires both variables.
- 77 (2) Then, the binary datasets are compared against each other and with the E-NRTL model with  
78 preliminary parameters. Doing so, inconsistent datasets are spotted as they do not agree with  
79 data from multiple other sources (for binary mixtures, the data status is quite extensive, and  
80 there are always datasets from multiple sources that agree with each other), and are removed.  
81 The remaining datasets constitute the benchmark database of the binary mixtures.
- 82 (3) Based on these datasets, parameters are regressed for the water-alcohol and water-salt pairs.  
83 Once these parameters (water-alcohol and water-salt) are sufficiently validated, they are used  
84 in the evaluation of the ternary (water + alcohol + salt) datasets, along with preliminary  
85 parameters for the alcohol-salt pairs. Because the solubility of salts in anhydrous alcohol is

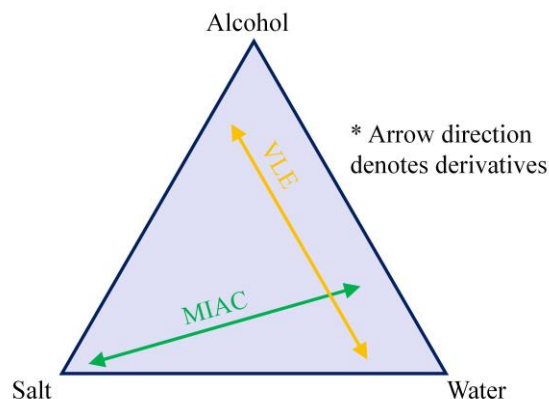
86 usually very small, in which range the model is dominated by the Pitzer-Debye-Huckel (PDH)  
 87 term, regression of the parameters of the alcohol-salt pairs to binary (alcohol + salt) data is  
 88 infeasible. Mixed-solvent electrolyte solution data are more suitable for obtaining alcohol-salt  
 89 parameters. Therefore, the binary (alcohol + salt) mixtures are not included in this benchmark  
 90 database. Compared to the data status of the aqueous electrolyte solutions, that of the mixed-  
 91 solvent electrolyte solutions is not as extensive. The datasets are evaluated by comparing with  
 92 other datasets for the same mixture when they are available, and by observing the data trends  
 93 to identify obvious outliers. Inconsistent datasets are identified and removed. The remaining  
 94 datasets are further marked as “recommended”, “tentative”, and “uncertain”, constituting the  
 95 benchmark database of the mixed-solvent electrolyte solutions. Based on the database,  
 96 parameters of the E-NRTL model are regressed.



97  
 98 Figure 1. Data analysis framework.

99 **2.1 Properties and their relationships with the activity coefficients**

100 MIAC and VLE include information about the derivatives of the excess Gibbs energy ( $G^E$ )  
 101 with respect to salt and solvent molar fractions, as shown in Figure 2. The arrow direction denotes  
 102 that the composition derivatives of  $G^E$  are for the corresponding components. By definition, MIAC  
 103 relates to the derivative of  $G^E$  over the salt composition, while VLE relates to the derivative of  $G^E$   
 104 over the solvent compositions. Therefore, they are ideal for model parameterization, and are  
 105 included in the database.



106  
107 Figure 2. Schematics of the correspondence between the properties and composition derivatives of  $G^E$ .

108 The activity coefficient describes deviation from ideality based on a given reference state and  
109 composition unit. For ions, a common convention of the activity coefficient is the rational  
110 asymmetrical activity coefficient. For aqueous electrolyte solutions, the ionic activity coefficient  
111 is normalized at infinite dilution in the water solvent. For mixed-solvent electrolyte solutions, the  
112 ionic activity coefficient is normalized at infinite dilution in the solvent mixture at the same salt-  
113 free composition, because, otherwise, large experimental composition uncertainties would be  
114 present at low water composition when properties are defined in the molality unit. In the  
115 experimental literature, data are always reported based on the molality unit defined in the solvent  
116 mixture.

$$\gamma_i^* = \frac{\gamma_i}{\gamma_i^\infty} \quad (1)$$

117 where  $\gamma_i$  is the symmetrical activity coefficient,  $\gamma_i^\infty$  is  $\gamma_i$  at infinite dilution in the solvent mixture  
118 at the corresponding salt-free composition. Thus, the reference state in Eq. (1) is different according  
119 to the salt-free composition of the solvent mixture. However, the rational asymmetrical activity  
120 coefficient, as well as the molality and molarity conventions, are only used for presentation; while  
121  $\gamma_i$  itself is calculated in the models. In this work, unless otherwise noted, the reference state of ionic  
122 activity coefficient is defined at infinite dilution in the solvent mixture.

123 In addition, the molality activity coefficient ( $\gamma_i^m$ ) and molarity activity coefficient ( $\gamma_i^c$ ) are  
124 also widely used conventions:

$$\gamma_i^m = \gamma_i^* \sum_j^{\text{solvents}} x_j \quad (2)$$

$$\gamma_i^c = \gamma_i^* \frac{\rho_{\text{solvent}}}{\rho_{\text{solution}}} \quad (3)$$

125 where  $\rho$  is the mass density. Like  $\gamma_i^*$ ,  $\gamma_i^m$  and  $\gamma_i^c$  also take reference state at infinite dilution in the  
 126 solvent mixture at the corresponding salt-free composition.

127 The MIAC is usually reported in the experimental literature in the molality convention.

$$\gamma_{\pm}^m = (\gamma_c^{m\nu_c} \gamma_a^{m\nu_a})^{\frac{1}{\nu}} \quad (4)$$

128 where  $\nu = \nu_c + \nu_a$  is the sum of the stoichiometric coefficients, the subscript c denotes cations,  
 129 and the subscript a denotes anions.

130 The MIAC is usually measured using potentiometry (also noted as electromotive force  
 131 measurement) <sup>41</sup>. An alternative approach is to calculate MIAC based on the Gibbs-Duhem  
 132 equation, e.g., the isopiestic vapor pressure measurements conducted by Robinson and co-workers  
 133 for many aqueous solutions <sup>42-44</sup>. However, for mixed-solvent electrolyte solutions, an infinite  
 134 dilution activity coefficient model is needed for converting the reference state of these data to the  
 135 infinite dilution of the salt in the solvent mixture at the same salt-free solvent composition. In this  
 136 work, all the collected data are measured by potentiometry. This reflects what has been  
 137 unanimously implemented in the experimental community. In the potentiometric measurements,  
 138 the electromotive force of the cells are measured, and substituted into the Nernst equation as a  
 139 function of molality (defined in the solvent mixture) along with an activity coefficient model, e.g.,  
 140 the extended Debye-Hückel. With some treatment, the expression is close to linear with molality  
 141 <sup>13,45</sup>. Coefficients of the Nernst equation and the activity coefficient model are regressed at the same  
 142 time for each salt-free composition. The obtained coefficients are then used for calculating the  
 143 MIAC. Thus, the reported MIAC depends not only on the measurement of the particular salt  
 144 molality, but also on the series of measurements for the salt-free solvent composition.

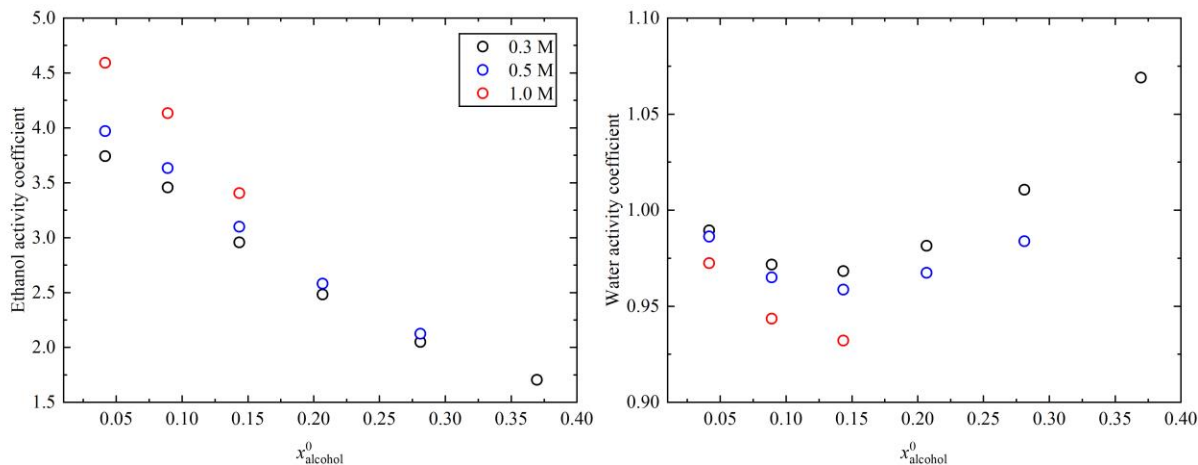
145 In the experimental literature, the uncertainty of electromotive force measurement, rather than  
 146 of the MIAC itself, is usually reported. The electromotive force can be measured up to very high  
 147 accuracy, e.g., 0.02 mV, corresponding to 0.05% in the MIAC <sup>41</sup>. However, the abovementioned  
 148 data treatment procedure introduces uncertainty in the obtained MIAC. Furthermore, the  
 149 measurement uncertainties of composition and temperature also contribute to the combined  
 150 uncertainty of the MIAC. For mixed-solvent electrolyte solutions, the relatively large deviations (in

151 some cases more than 20%) observed in mixed-solvent electrolyte measurements from different  
 152 experimental sources is a matter of reliability rather than accuracy, indicating an imperative need  
 153 for critically evaluating the data before use in model developments.

154 When the mixed-solvent electrolyte solution VLE data include both vapor pressure and vapor  
 155 phase molar fraction, the solvent activity coefficient can be obtained taking the ideal gas  
 156 assumption in the vapor phase,

$$\gamma_{i,\text{solvent}} = \frac{y_{i,\text{solvent}}p}{x_{i,\text{solvent}}p_{i,\text{solvent}}^{\text{sat}}} \quad (5)$$

157 where  $y$  is the molar fraction in the vapor phase,  $x$  is the molar fraction in the liquid phase,  $p$  is the  
 158 pressure,  $p_{i,\text{solvent}}^{\text{sat}}$  is the vapor pressure of pure solvent  $i$  at the temperature. Eq. (5) assumes that  
 159 the pressure is sufficiently small so that the vapor phase can be treated as ideal gas and that no  
 160 Poynting correction is needed in the liquid phase. Figure 3 shows the solvent activity coefficients  
 161 derived from experimental VLE data for (water + ethanol + KCl) at 298.15 K using Eq. (5). As salt  
 162 composition increases, alcohol activity coefficient increases, while water activity coefficient  
 163 decreases. The alcohol activity coefficient changes more with the salt composition at low alcohol  
 164 composition, while the water activity coefficient is close to unity in the entire experimental data  
 165 range. As alcohol composition increases, alcohol activity coefficient decreases, while water activity  
 166 coefficient first decreases and then increases.



167  
 168 Figure 3. Solvent activity coefficients derived from experimental VLE data<sup>46</sup> for (water + ethanol + KCl)  
 169 at 298.15 K.

170 The ionic and solvent activity coefficients are related to each other according to the Gibbs-  
 171 Duhem equation. At constant  $T$  and  $p$ ,



$$\sum n_{i,\text{solv}} d \ln x_{i,\text{solv}} \gamma_{i,\text{solv}} + n_s \sum \nu d \ln m_{\pm} \gamma_{\pm}^m = 0 \quad (6)$$

172 Therefore, MIAC and VLE are complementary to each other. Experimental data of these  
173 properties can be utilized to verify each other.

## 174 2.2 Composition denotations

175 Experimental data were reported in many different conventions. Typically, for mixed-solvent  
176 electrolyte mixtures, solvent compositions were usually reported in molar fraction or weight  
177 fraction on the salt-free basis, while salt compositions were usually reported in molar fraction,  
178 molality, or molarity. Before any modeling work, these data need to be converted to the same unit,  
179 typically ion-based molar fraction, which is used in most models. For instance, the composition  
180 unit of salt-free molar fraction for solvent and molality for salt can be converted to ion-based molar  
181 fraction according to,

$$x_{i,\text{solvent}} = \frac{1000 \text{ g} \times \sum_j \frac{x_{j,\text{solvent}}^0}{M_{j,\text{solvent}}}}{\nu x_{\text{salt}}^0 + 1000 \text{ g} \times \sum_j \frac{x_{j,\text{solvent}}^0}{M_{j,\text{solvent}}}} \quad (7)$$

$$x_{i,\text{ion}} = \frac{\nu_i x_{\text{salt}}^0}{\nu x_{\text{salt}}^0 + 1000 \text{ g} \times \sum_j \frac{x_{j,\text{solvent}}^0}{M_{j,\text{solvent}}}} \quad (8)$$

182 where  $x^0$  is in the original composition unit before conversion,  $M$  is the molar mass, and the  
183 subscript ion denotes cation or anion. In this work, we consider only the alkali halides. Hence,  $\nu =$   
184 2,  $\nu_i = 1$ .

## 185 2.3 Raw data collected from databanks

186 Data are collected from DETHERM<sup>47</sup>, CERE electrolyte databank<sup>48</sup>, and other sources, e.g.,  
187 datasets that were utilized in other modeling papers (e.g., references<sup>16,19,21,23–25</sup>), etc. All the  
188 collected data are experimental and available in public literature. Datasets that are not provided in  
189 tabular forms are excluded. VLE datasets that do not report both vapor pressure and vapor phase  
190 molar fraction are excluded. Among those mixtures, experimental data are more extensive for the  
191 mixtures containing  $\text{Na}^+$  salts and  $\text{Cl}^-$  salts. Overall, the data status of the mixed-solvent electrolyte  
192 mixtures is much less extensive compared to that of aqueous alkali halide mixtures<sup>14</sup>. Data of the

193 constituting (alcohol + salt) binary mixtures are not included in the database, because the data status  
 194 is even scarcer compared to that of the mixed-solvent electrolyte solutions, because that MIAC  
 195 data is almost nonexistent, and because salt solubility is very small in alcohols in most cases.

196 After collecting the raw database and evaluating the data quality, a final database is  
 197 constructed by introducing some codes (“R” for “recommended”, “T” for “tentative”, and “U” for  
 198 “uncertain”). Details will be explained in Section 6.

## 199 2.4 Statistical quantities’ definitions

200 In what follows, the data will be compared with calculation results, resulting in the need for  
 201 defining some statistical quantities.

202 **Average deviation (AD) and maximum deviation (MD):** AD and MD represent deviations  
 203 of the model from each experimental dataset. For vapor pressure, the relative deviation is taken.  
 204 For vapor phase molar fraction and MIAC, the absolute deviation is taken. The vapor phase molar  
 205 fraction is between 0 and 1, while MIAC is in general between 0 and 1 in the salt composition  
 206 range that is used in the parameter optimization in this work. Using the absolute deviation rather  
 207 than the relative deviation avoids exaggerating the deviations when the values are small. In the data  
 208 analysis,  $x_{ion}$  is limited to 0.06, in which range MIAC is never much larger than 1. However, if  
 209 MIAC gets very large in the regression data, relative deviation should be used.

210 **Objective function (OF):** Parameters are optimized using a local minimizer in IFPEN’s  
 211 optimization software, ATOUT<sup>49</sup>, starting from the optimal value from 50 initial parameter sets  
 212 randomly obtained in the parameter ranges using a Latin hypercube algorithm. The combined  
 213 objective function (OF) is,

$$\begin{aligned}
 \text{OF} = & \frac{1}{2} \sum_{j=1}^{n_{\text{ds}}} \frac{\sum_{i=1}^{n_{\text{dp}}^j} (\gamma_{\text{cal}}^{\pm i,j} - \gamma_{\text{exp}}^{\pm i,j})^2}{n_{\text{dp}}^j} + \frac{1}{2} \sum_{j=1}^{n_{\text{ds}}} \frac{\sum_{i=1}^{n_{\text{dp}}^j} \left( \frac{p_{\text{cal}}^{i,j} - p_{\text{exp}}^{i,j}}{p_{\text{exp}}^{i,j}} \right)^2}{n_{\text{dp}}^j} \\
 & + \frac{1}{2} \sum_{j=1}^{n_{\text{ds}}} \frac{\sum_{i=1}^{n_{\text{dp}}^j} (y_{\text{cosolvent,cal}}^{i,j} - y_{\text{cosolvent,exp}}^{i,j})^2}{n_{\text{dp}}^j}
 \end{aligned} \tag{9}$$

214 where  $n_{ds}$  is the number of datasets,  $n_{dp}^j$  is the number of data points in dataset  $j$ , the subscript cal  
215 denotes calculated values, and the subscript exp denotes experimental values. Depending on the  
216 data status, MIAC and VLE are used individually or together for the different mixtures. In the  
217 following sections, the OF that only consists of MIAC data is denoted as OF-M, the OF that only  
218 consists of VLE data (pressure and vapor phase molar fraction) is denoted as OF-V, and the OF  
219 that consists of both MIAC and VLE is denoted as OF-MV. Quite often, uncertainty is not reported  
220 in the experimental literature. In addition, the uncertainty might be reported more optimistically in  
221 some experimental literature than others. Instead of using directly the data uncertainty as reported,  
222 a more rigorous approach is to adjust its value based on data distribution, observed deviation after  
223 correcting systematic deviations, and model capability<sup>50</sup>. However, the availability of experimental  
224 data and uncertainty of the mixed-solvent electrolyte solutions does not facilitate such detailed  
225 analysis. Therefore, the data uncertainty is not included in the data analysis. Instead, the same  
226 weight is assigned to all the datasets that are considered to be reliable after extensive comparisons  
227 between datasets from different experimental sources.

### 228 **3 Model for data analysis**

229 The electrolyte non-random two-liquid (E-NRTL) model<sup>51,52</sup> is used for data analysis because  
230 of its wide acceptance in the industry<sup>53</sup>, its capacity to describe mixed-solvent electrolyte solutions  
231<sup>27</sup>, its small number of adjustable parameters, and its potential theoretical basis of parameters<sup>54</sup>.  
232 The E-NRTL model includes a NRTL part<sup>55</sup>, which accounts for the local interaction contribution  
233 between all interacting species, and a PDH part<sup>56</sup>, which accounts for the long-range Coulombic  
234 interaction contribution between ions. Mock et al.<sup>26</sup> applied the E-NRTL model on mixed-solvent  
235 electrolyte mixtures, which was implemented in ASPEN PLUS. However, according to these  
236 authors, “only the local interaction contribution term of the electrolyte NRTL model is used in this  
237 study and the long-range interaction contribution term is dropped”, because their “main  
238 consideration was the ability to represent the phase equilibrium behavior of solvent species”. The  
239 model was successful in representing VLE. Liu and Watanasiri<sup>57</sup> introduced a Bronsted-  
240 Guggenheim term<sup>39,40</sup> and a Born term<sup>58,59</sup> into the model, and applied the E-NRTL model on the  
241 representation of liquid-liquid equilibrium of mixed-solvent electrolyte solutions. Van Bochove et  
242 al.<sup>31</sup> suggested that the difference in the dielectric constants of the solvents were large in the (water  
243 + organic solvent + salt) mixtures, and included the correct solvent composition derivatives in their

244 PDH and Born terms. The resulting E-NRTL model satisfies the Gibbs-Duhem equation, and thus  
 245 is consistent. However, they suggested that the consistent e-NRTL is only slightly better than  
 246 original e-NRTL. In a recent work, Chang and Lin<sup>60</sup> included the ion contribution to the solvent-  
 247 related properties in their extended PDH model. However, van Bochove's derivations were largely  
 248 ignored in later works on mixed-solvent electrolyte modeling with the E-NRTL model. The Born  
 249 term<sup>58,59</sup> in the E-NRTL model accounts for the difference of medium effect between the infinite-  
 250 dilution aqueous solution to the given mixed-solvent solution. Song and Chen<sup>27</sup> proposed a  
 251 segmental E-NRTL model for mixed-solvent electrolyte solutions, and later proposed a  
 252 symmetrical version<sup>61</sup> to accommodate pure fused salts. In these works, the solvent density and  
 253 relative permittivity were considered as pseudo-pure functions, i.e., although solvent-composition  
 254 dependence was accounted for in the function, derivative terms were omitted as activity  
 255 coefficients were derived from the excess Gibbs energy. Tsanas et al.<sup>62</sup> suggested that violation of  
 256 the Gibbs-Duhem equation would result in convergence to the wrong minimum in reactive flash  
 257 calculations. In this section, the consistent E-NRTL model is described; then, the consistent and  
 258 original E-NRTL models are compared to show whether the issue of consistency matters for VLE  
 259 and MIAC calculations, which are the scope of the presented database in this work.

### 260 **3.1 Consistent E-NRTL**

261 For mixed-solvent electrolyte solutions, the original E-NRTL<sup>27,61</sup> is usually used in a manner  
 262 that violates the Gibbs-Duhem equation. (The problem is not present for single-solvent systems.)  
 263 In Van Bochove et al.'s work<sup>31</sup>, the model satisfies the Gibbs-Duhem equation, and therefore is  
 264 consistent. In the consistent E-NRTL model, the PDH and Born terms are different from the  
 265 original E-NRTL, as the correct solvent composition derivatives are included. This work utilizes a  
 266 model that is similar to Van Bochove's consistent model, short of the Bronsted-Guggenheim term.  
 267 The model consists of a NRTL term, a PDH term, and a Born term. Here, the model is briefly  
 268 introduced.

269 The activity coefficient terms are obtained by taking partial derivatives of the excess Gibbs  
 270 energy terms:

$$\frac{G^{E,PDH}}{RT} = - \left( \sum_i n_i \right) \frac{4A_\phi I_x}{\rho} \ln \left( 1 + \rho I_x^{\frac{1}{2}} \right) \quad (10)$$

$$\frac{G^{\text{E,Born}}}{RT} = \frac{Q_e^2}{2kT} \left( \frac{1}{\varepsilon_s \varepsilon_0} - \frac{1}{\varepsilon_w \varepsilon_0} \right) \sum \frac{n_i Z_i^2}{r_i} \quad (11)$$

271 where  $R = 8.3144598 \text{ J mol}^{-1} \text{ K}^{-1}$  is the universal gas constant<sup>63</sup>,  $T$  is the temperature,  $n_i$  is the  
 272 molar number of component  $i$ ,  $A_\varphi$  is one third of the Debye-Huckel limiting slope as given in Eq.  
 273 (12),  $I_x$  is the ionic strength as given in Eq. (13),  $Q_e = 1.6021766208 \times 10^{-19} \text{ C}$  is the  
 274 elementary charge<sup>63</sup>,  $k = 1.38064852 \times 10^{-23} \text{ m}^2 \text{ kg s}^{-2} \text{ K}^{-1}$  is the Boltzmann constant<sup>63</sup>,  $\varepsilon_s$  is  
 275 the solvent relative permittivity,  $\varepsilon_w$  is the water relative permittivity,  $\varepsilon_0 = 8.854187817 \times$   
 276  $10^{-12} \text{ F m}^{-1}$  is the dielectric constant in the vacuum<sup>63</sup>,  $Z_i$  is the ionic charge,  $r_i$  is the Born radius  
 277 and is set at  $3 \text{ \AA}$  for all the ions in this work.

$$A_\varphi = \frac{1}{3} \left( \frac{2\pi N_A \rho_s}{1000} \right)^{\frac{1}{2}} \left( \frac{25Q_e^2}{\pi \varepsilon_s \varepsilon_0 kT} \right)^{\frac{3}{2}} \quad (12)$$

$$I_x = \frac{\sum Z_i^2 n_i}{2 \sum n_i} \quad (13)$$

278 where  $N_A = 6.022140857 \times 10^{23} \text{ mol}^{-1}$  is the Avogadro number<sup>63</sup>.

279 The mixing rules for solvent density and relative permittivity are,

$$\rho_s = \frac{1}{\sum_i^{\text{solvents}} \frac{x_i^0}{\rho_i}} \quad (14)$$

$$\varepsilon_s = \sum_i^{\text{solvents}} w_i^0 \varepsilon_i \quad (15)$$

280 where  $x_i^0$  is the molar fraction on the salt-free basis,  $w_i^0$  is the weight fraction on the salt-free basis,  
 281  $\rho_i$  is the density of solvent  $i$ , and  $\varepsilon_i$  is the relative permittivity of solvent  $i$ , as given below.

$$\rho_i = \frac{A_i}{B_i^{1 + \left(1 - \frac{T}{C_i}\right)^{D_i}}} \quad (16)$$

$$\varepsilon_i = \varepsilon_i^0 + \varepsilon_i^1 \left( \frac{1}{T} - \frac{1}{273.15 \text{ K}} \right) \quad (17)$$

282 The coefficients,  $A_i$ ,  $B_i$ ,  $C_i$ ,  $D_i$ ,  $\varepsilon_i^0$  and  $\varepsilon_i^1$ , are obtained from or regressed to data from DIPPR<sup>64</sup> and  
 283 reference<sup>65</sup>, as explained in detail in the Supporting Information.

284 Thus, the activity coefficient terms are,

$$\begin{aligned}
\ln \gamma_i^{\text{PDH}} &= \left[ \frac{\partial \left( \frac{G^{\text{E,PDH}}}{RT} \right)}{\partial n_i} \right]_{T,p,n_j(j \neq i)} \\
&= \frac{G^{\text{E,PDH}}}{RT} \left\{ \frac{1}{\sum_k n_k} + \frac{1}{A_\varphi} \left( \frac{\partial A_\varphi}{\partial n_i} \right)_{T,p,n_j(j \neq i)} \right. \\
&\quad \left. + \frac{1}{I_x} \left( \frac{\partial I_x}{\partial n_i} \right)_{T,p,n_j(j \neq i)} \left[ 1 + \frac{1}{2 \left( 1 + \rho^{-1} I_x^{-\frac{1}{2}} \right) \ln \left( 1 + \rho I_x^{\frac{1}{2}} \right)} \right] \right\}
\end{aligned} \tag{18}$$

$$\begin{aligned}
\ln \gamma_i^{\text{Born}} &= \left[ \frac{\partial \left( \frac{G^{\text{E,Born}}}{RT} \right)}{\partial n_i} \right]_{T,p,n_j(j \neq i)} \\
&= \begin{cases} -\frac{Q_e^2}{2kT \varepsilon_s^2 \varepsilon_0} \left( \frac{\partial \varepsilon_s}{\partial n_i} \right)_{T,p,n_j(j \neq i)} \left( \sum \frac{n_k Z_k^2}{100 r_k} \right) & \text{for solvents} \\ \frac{Q_e^2}{2kT} \left( \frac{1}{\varepsilon_s \varepsilon_0} - \frac{1}{\varepsilon_w \varepsilon_0} \right) \frac{Z_i^2}{100 r_i} & \text{for ions} \end{cases}
\end{aligned} \tag{19}$$

285 where the analytical expressions for  $\left( \frac{\partial A_\varphi}{\partial n_i} \right)_{T,p,n_j(j \neq i)}$  and the other derivatives over  $n_i$  are provided

286 in the Supporting Information.

287 The 2nd term in Eq. (18) and the upper equation in Eq. (19) are not included in the original  
288 E-NRTL, as derivatives of solvent density and relative permittivity over solvent composition are  
289 ignored. As these terms are included, the Gibbs-Duhem equation, which is violated by the original  
290 E-NRTL, is satisfied. Consequently, in principle, one can expect that the consistent E-NRTL can  
291 reconcile the ion and solvent properties (MIAC and VLE) better.

292 The consistent E-NRTL model uses exactly the same formulation for the NRTL term as the  
293 original E-NRTL<sup>51,52</sup>.

$$\begin{aligned}
\ln \gamma_m^{\text{NRTL}} &= \frac{\sum_j x_j G_{jm} \tau_{jm}}{\sum_j x_j G_{jm}} + \sum_{m'} \frac{x_{m'} G_{mm'}}{\sum_k x_k G_{km'}} \left( \tau_{mm'} - \frac{\sum_k x_k G_{km'} \tau_{km'}}{\sum_k x_k G_{km'}} \right) \\
&+ \sum_c \frac{\frac{\sum_{a'} x_{a'} x_c G_{mc,a'c}}{\sum_k x_k G_{kc,a'c}} \left( \tau_{mc,a'c} - \frac{\sum_{k \neq c} x_k G_{kc,a'c} \tau_{kc,a'c}}{\sum_{k \neq c} x_k G_{kc,a'c}} \right)}{\sum_{a''} x_{a''}} \\
&+ \sum_a \frac{\frac{\sum_{c'} x_{c'} x_a G_{ma,c'a}}{\sum_k x_k G_{ka,c'a}} \left( \tau_{ma,c'a} - \frac{\sum_{k \neq a} x_k G_{ka,c'a} \tau_{ka,c'a}}{\sum_{k \neq a} x_k G_{ka,c'a}} \right)}{\sum_{c''} x_{c''}}
\end{aligned} \tag{20}$$

$$\begin{aligned}
\frac{\ln \gamma_c^{\text{NRTL}}}{Z_c} &= \frac{\sum_{a'} \frac{x_{a'} \sum_k x_k G_{kc,a'c} \tau_{kc,a'c}}{\sum_k x_k G_{kc,a'c}}}{\sum_{a''} x_{a''}} + \sum_m \frac{x_m G_{cm}}{\sum_k x_k G_{km}} \left( \tau_{cm} - \frac{\sum_k x_k G_{km} \tau_{km}}{\sum_k x_k G_{km}} \right) \\
&+ \sum_a \frac{\frac{\sum_{c'} x_{c'} x_a G_{ca,c'a}}{\sum_k x_k G_{ka,c'a}} \left( \tau_{ca,c'a} - \frac{\sum_{k \neq a} x_k G_{ka,c'a} \tau_{ka,c'a}}{\sum_{k \neq a} x_k G_{ka,c'a}} \right)}{\sum_{c''} x_{c''}}
\end{aligned} \tag{21}$$

$$\begin{aligned}
\frac{\ln \gamma_a^{\text{NRTL}}}{Z_a} &= \frac{\sum_{c'} \frac{x_{c'} \sum_k x_k G_{ka,c'a} \tau_{ka,c'a}}{\sum_k x_k G_{ka,c'a}}}{\sum_{c''} x_{c''}} + \sum_m \frac{x_m G_{am}}{\sum_k x_k G_{km}} \left( \tau_{am} - \frac{\sum_k x_k G_{km} \tau_{km}}{\sum_k x_k G_{km}} \right) \\
&+ \sum_c \frac{\frac{\sum_{a'} x_{a'} x_c G_{ac,a'c}}{\sum_k x_k G_{kc,a'c}} \left( \tau_{ac,a'c} - \frac{\sum_{k \neq c} x_k G_{kc,a'c} \tau_{kc,a'c}}{\sum_{k \neq c} x_k G_{kc,a'c}} \right)}{\sum_{a''} x_{a''}}
\end{aligned} \tag{22}$$

294 where,

$$\tau_{ma,ca} = \tau_{am} - \tau_{ca,m} + \tau_{m,ca} \tag{23}$$

$$\tau_{am} = -\ln \frac{G_{am}}{\alpha_{am}} \tag{24}$$

$$G_{am} = \frac{\sum_c x_c G_{ca,m}}{\sum_c x_c} \tag{25}$$

$$\alpha_{am} = \frac{\sum_c x_c \alpha_{ca,m}}{\sum_c x_c} \tag{26}$$

$$\tau_{mc,ac} = \tau_{cm} - \tau_{ca,m} + \tau_{m,ca} \tag{27}$$

$$\tau_{cm} = -\ln \frac{G_{cm}}{\alpha_{cm}} \tag{28}$$

$$G_{cm} = \frac{\sum_a x_a G_{ca,m}}{\sum_a x_a} \tag{29}$$

$$\alpha_{cm} = \frac{\sum_a x_a \alpha_{ca,m}}{\sum_a x_a} \quad (30)$$

$$G = e^{-\alpha\tau} \quad (31)$$

295 Eqs. (18), (19), (21), and (22) are in the symmetrical convention. For ions, they can be  
 296 converted into the rational unsymmetrical and molality conventions according to Eqs. (1) and (2).

297 The  $\alpha$  parameters are interchangeable, i.e.,  $\alpha_{ij} = \alpha_{ji}$ . In this work, there are only one cation and  
 298 one anion in each mixture. Thus, the salt-salt parameters,  $\tau_{ca,c'a} = \tau_{ca,c'}$  and  $\tau_{ac,a'c} = \tau_{ac,a'}$ , are  
 299 not relevant here. The adjustable parameters are  $\alpha_{\text{water,alcohol}}$ ,  $\alpha_{\text{water,salt}}$ ,  $\alpha_{\text{alcohol,salt}}$ ,  $\tau_{\text{water,alcohol}}$ ,  
 300  $\tau_{\text{alcohol,water}}$ ,  $\tau_{\text{water,salt}}$ ,  $\tau_{\text{salt,water}}$ ,  $\tau_{\text{alcohol,salt}}$ , and  $\tau_{\text{alcohol,salt}}$ . In short, these parameters are noted as  $\alpha_{wa}$ ,  $\alpha_{ws}$ ,  
 301  $\alpha_{as}$ ,  $\tau_{wa}$ ,  $\tau_{aw}$ ,  $\tau_{ws}$ ,  $\tau_{sw}$ ,  $\tau_{as}$ , and  $\tau_{as}$ .  $\alpha_{wa} = 0.3$ ,  $\alpha_{ws} = 0.2$ , and  $\alpha_{as} = 0.2$  are taken according to common  
 302 practice<sup>27</sup>. There is no adjustable parameter in the PDH and Born terms. Therefore, the remaining  
 303 adjustable parameters are the  $\tau$  parameters. In addition, a temperature dependence is introduced for  
 304  $\tau$ :

$$\tau = \tau_0 + \tau_1 \left( \frac{1}{T} - \frac{1}{T_0} \right) \quad (32)$$

305 where  $\tau_0$  is obtained at  $T_0$ , at which isothermal datasets are usually available, typically at 298.15  
 306 K, while  $\tau_1$  is obtained with datasets at other temperatures.

### 307 3.2 Is consistency an issue?

308 Because that the difference between the consistent and original E-NRTL models is only with  
 309 solvent composition derivatives, and that MIAC only involves ion composition derivatives, the  
 310 consistent modification has no impact on MIAC. Thus, the parameters of the consistent and original  
 311 E-NRTL models are identical for OF-M. Table 1 shows the ADs and MDs of the consistent and  
 312 original E-NRTL models with OF-M and OF-MV. For vapor pressure, the relative deviation is  
 313 taken (see Eq. (9)). For vapor phase molar fraction and MIAC, the absolute deviation is taken,  
 314 because these data are in general between 0 and 1, and thus the relative deviations are exaggerated  
 315 when the values are small. In the cases with OF-M, VLE is predicted. For the methanol mixtures,  
 316 with OF-M, the consistent E-NRTL model predicts both VLE  $p$  and  $y$  more accurately than the  
 317 original model; with OF-MV, there is no significant difference between the consistent and original  
 318 E-NRTL models. For the ethanol mixtures, however, with either OF-M or OF-MV, the difference



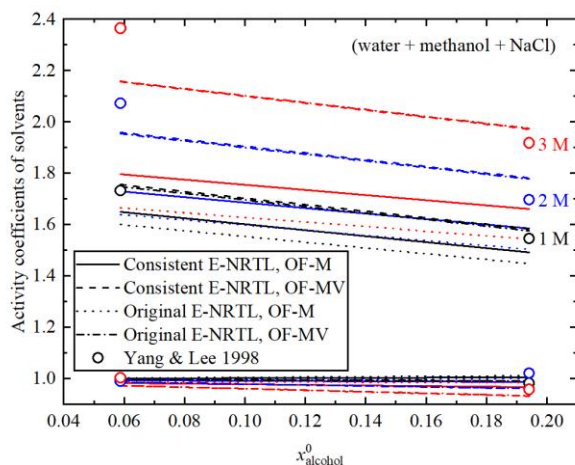
319 between the consistent and original E-NRTL models is not significant in terms of the ADs and  
320 MDs of MIAC and VLE.

321 Table 1. Average deviations (ADs) and maximum deviations (MDs) of the consistent and original E-NRTL models with OF-M (MIAC) and OF-MV (MIAC and  
322 VLE). The prediction deviations are presented in italic and blue. Temperature and composition ranges of the experimental datasets are provided in Table 4. Ion  
323 composition is cut off at  $x_{\text{ion}} = 0.06$ .

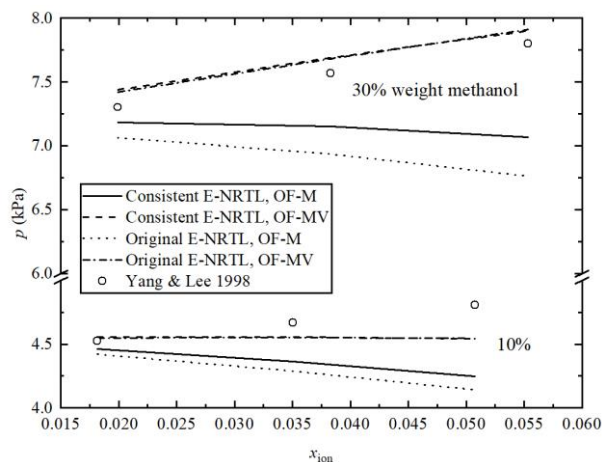
Mixture	Property	Reference	Consistent, OF-M		Consistent, OF-MV		Original, OF-M		Original, OF-MV	
			100AD	100MD	100AD	100MD	100AD	100MD	100AD	100MD
(water + methanol + NaCl)	MIAC	Xu et al. 2014 <sup>66</sup>	0.56	1.4	0.60	1.4	0.56	1.4	0.64	1.5
		Basili et al. 1996 <sup>67</sup>	1.4	5.0	1.5	6.0	1.4	5.0	1.5	6.7
	VLE	Yang & Lee 1998 <sup>68</sup> , <i>p</i> <i>y</i>	<i>6.0</i>	<i>12</i>	2.2	5.5	<i>8.2</i>	<i>14</i>	2.2	5.5
(water + methanol + KCl)	MIAC	Basili et al. 1997 <sup>69</sup>	1.1	4.2	1.2	4.5	1.1	4.2	1.2	4.6
		VLE	Yang & Lee 1998 <sup>68</sup> , <i>p</i> <i>y</i>	<i>3.3</i>	<i>7.4</i>	1.8	4.3	<i>4.5</i>	<i>8.7</i>	1.7
	MIAC	Esteso et al. 1989 <sup>70</sup> Mamontov et al. 2016 <sup>71</sup> <sup>a</sup>	2.4	7.2	2.4	7.2	2.4	7.2	2.5	7.3
(water + ethanol + NaCl)	MIAC	Esteso et al. 1989 <sup>70</sup>	2.4	7.2	2.4	7.2	2.4	7.2	2.5	7.3
		Mamontov et al. 2016 <sup>71</sup> <sup>a</sup>	0.91	2.7	0.91	2.9	0.91	2.7	1.0	3.5
	VLE	Yang et al. 1979 <sup>46</sup> , <i>p</i> <i>y</i>	<i>2.1</i>	<i>5.5</i>	2.2	6.5	<i>1.8</i>	<i>4.4</i>	2.0	6.0
(water + ethanol + KCl)	MIAC	Mussini et al. 1995 <sup>72</sup>	0.88	1.7	0.88	1.8	0.88	1.7	0.90	1.7
		VLE	Yang et al. 1979 <sup>46</sup> , <i>p</i> <i>y</i>	<i>2.0</i>	<i>3.7</i>	2.4	4.0	<i>0.98</i>	<i>2.6</i>	2.3
	MIAC	Mussini et al. 1995 <sup>72</sup>	0.88	1.7	0.88	1.8	0.88	1.7	0.90	1.7

324 Note: <sup>a</sup> The dataset includes data at other temperatures. Deviations in this table are for the 298.15 K part of the dataset.

325 However, the more significant differences in trends are masked by the AD and MD values.  
326 Figure 4 shows the comparison of the solvent activity coefficients of (water + methanol + NaCl)  
327 calculated using the consistent and original E-NRTL models with OF-M and OF-MV. The line  
328 types denote the different models. The colors denote the salt compositions. The lines and dots in  
329 the upper part of the graph are alcohol activity coefficient, while those in the lower part are water  
330 activity coefficient. The latter is close to unity for all the mixtures in the entire data ranges, and  
331 does not represent a good criterion against the models. Thus, here the analysis focuses on the  
332 alcohol activity coefficient. Figures for (water + methanol + KCl), (water + ethanol + NaCl/KCl)  
333 are provided in the Supporting Information. With OF-MV, the results calculated with the consistent  
334 and original E-NRTL models almost overlap. With OF-M, the results calculated with the consistent  
335 E-NRTL model is closer to the experimental data compared to the original model for all the  
336 mixtures. Therefore, although not to the level of the OF-MV results, VLE is predicted more  
337 accurately with the consistent model compared to the original model, when only MIAC is available,  
338 which is often the case as shown in the data summary in Section 6. A table is provided in the  
339 Supporting Information for the parameters. For all the mixtures, the parameters regressed with OF-  
340 M and OF-MV are closer for the consistent model compared to the original, which confirms that  
341 the MIAC and VLE properties are better reconciled when calculated using the consistent E-NRTL  
342 model. In addition, the alcohol activity coefficient of the methanol mixtures present larger  
343 deviations with OF-M. Figure 5 shows the vapor pressure of (water + methanol + NaCl) with 10%  
344 and 30% weight fraction methanol (salt-free basis) with OF-M and OF-MV at 298.15 K. As salt  
345 composition increases, the experimental vapor pressure increases, i.e., the salting out behavior  
346 dominates vapor pressure change even at this low alcohol composition; the consistent and original  
347 E-NRTL models with OF-MV capture this behavior; while the models with OF-M fail to capture  
348 this behavior, which results in the comparatively larger deviations as shown in Table 1.



349  
 350 Figure 4. Comparison of the solvent activity coefficients of (water + methanol + NaCl) calculated using  
 351 the consistent and original E-NRTL models with OF-M and OF-MV at 298.15 K. The upper part of the  
 352 graph is alcohol activity coefficient, while the lower part is water activity coefficient. The experimental  
 353 data is from reference <sup>68</sup>.



354  
 355 Figure 5. Vapor pressure of (water + methanol + NaCl) with 10% and 30% weight fraction methanol (salt-  
 356 free basis) with OF-M and OF-MV at 298.15 K. The experimental data is from reference <sup>68</sup>.

357 To sum up, with OF-MV, there is no significant difference between the consistent and original  
 358 E-NRTL models; with OF-M, the consistent E-NRTL model is more accurate than the original  
 359 model, in terms of both VLE results and trends of solvent activity coefficients. In the following  
 360 context, unless specifically noted, the consistent E-NRTL model is analyzed; “E-NRTL” refers to  
 361 the consistent model.

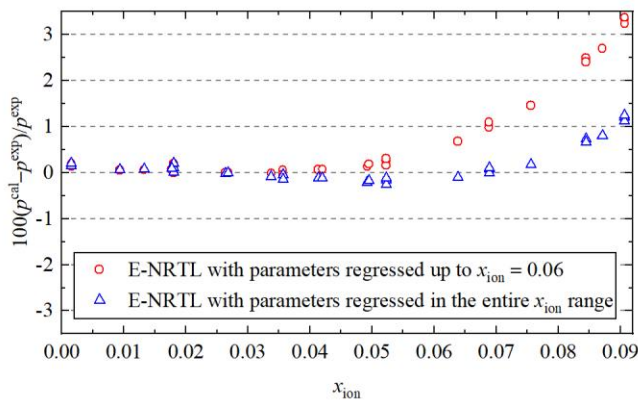
### 362 3.3 E-NRTL at larger salt composition

363 This section investigates how the E-NRTL model extrapolates to larger salt composition. The  
 364 aim is to find a cut-off salt composition that can be used in data selection, rather than to obtain

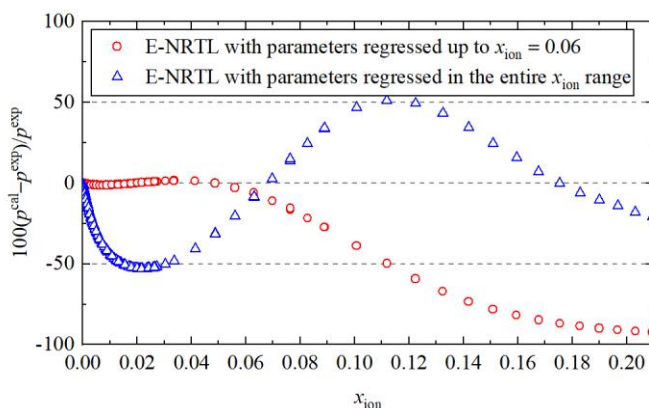
365 accurate results in as large range as possible. We find that the E-NRTL model is not accurate for  
366 both aqueous and mixed-solvent electrolyte solutions at large salt composition.

367 Results of (water + salt) binary mixtures are shown rather than those of (water + alcohol +  
368 salt) ternary mixtures, because the former are confirmed by experimental data from various sources.  
369 Figures 6 and 7 show the deviations of vapor pressure calculated with the E-NRTL model with OF-  
370 MV and parameters regressed in the region up to  $x_{\text{ion}} = 0.06$  and in the entire  $x_{\text{ion}}$  range for (water  
371 + NaCl) and (water + LiCl). Results for MIAC is not significantly different within  $x_{\text{ion}} = 0.06$  and  
372 is presented in the Supporting Information. References for the experimental datasets are provided  
373 in the Supporting Information. The red and blue dots are the same datasets compared with the E-  
374 NRTL model using different parameters. In this work, all electrolyte solution data (MIAC and VLE,  
375 aqueous and mixed-solvent) are cut off at  $x_{\text{ion}} = 0.06$  when parameters are regressed. There are  
376 three scenarios following this cut off. For salts with low solubility, e.g., KCl and NaF, the cut off  
377 covers all or most of the solubility range. Thus, the cut off  $x_{\text{ion}}$  is close to the solubility limit, i.e.,  
378 the parameters regressed up to  $x_{\text{ion}} = 0.06$  applies up to the solubility limit. For salts with  
379 solubility that is moderately larger than  $x_{\text{ion}} = 0.06$ , e.g., NaCl, MIAC and VLE calculated with  
380 parameters regressed up to  $x_{\text{ion}} = 0.06$  are slightly more accurate at lower salt composition  
381 compared to those calculated with parameters regressed in the entire  $x_{\text{ion}}$  range (approximately up  
382 to  $x_{\text{ion}} = 0.09$ ); however, deviations increase drastically beyond  $x_{\text{ion}} = 0.06$  and reach 0.15 at  
383  $x_{\text{ion}} = 0.09$ , while the deviation of MIAC calculated with parameters regressed in the entire  $x_{\text{ion}}$   
384 range is within 0.05 at  $x_{\text{ion}} = 0.09$ ; for vapor pressure, the increase of deviation is much smaller  
385 in the large  $x_{\text{ion}}$  range compared to that of MIAC, being slightly larger than 3% at the solubility  
386 limit. When regressed to MIAC and VLE data in the entire composition range, the obtained  
387 parameters are exactly the same as those reported by Yan and Chen<sup>73</sup>, i.e.,  $\tau_{\text{sw}} = -4.54$ ,  $\tau_{\text{ws}} = 8.86$ .  
388 For salts with solubility that is much larger than  $x_{\text{ion}} = 0.06$ , e.g., LiCl, however, although VLE  
389 is included in the objective function along with MIAC, regression in the entire  $x_{\text{ion}}$  range results  
390 in large deviation in vapor pressure (up to 50%) in both low and high salt composition ranges. To  
391 sum up, regression to the entire  $x_{\text{ion}}$  range can improve accuracy in the high salt composition range  
392 for salts with solubility that is moderately larger than  $x_{\text{ion}} = 0.06$ , but cannot for salts with  
393 solubility that is much larger than  $x_{\text{ion}} = 0.06$  (e.g., LiCl); in both cases, accuracy in the low salt  
394 composition range is worse compared to that calculated using parameters regressed up to  $x_{\text{ion}} =$

395 0.06. It is necessary to account for model capability when selecting the range of data used in  
 396 parameter regression rather than use everything available. Furthermore, salts present very different  
 397 solubility, while cutting off at certain  $x_{\text{ion}}$  provides a common ground that facilitates finding  
 398 parameter trends. Therefore, although the deviations are larger at the high salt composition for the  
 399 (water + NaCl) case, it is still decided that all data are cut off at  $x_{\text{ion}} = 0.06$ . The model is here  
 400 used to obtain a guide for data selection, rather than to obtain accurate results in large ranges.



401  
 402 Figure 6. Deviations from experimental data of vapor pressure calculated with the E-NRTL model with  
 403 OF-MV and parameters regressed in the region up to  $x_{\text{ion}} = 0.06$  and in the entire  $x_{\text{ion}}$  range for (water +  
 404 NaCl). References for the experimental datasets are provided in the Supporting Information.



405  
 406 Figure 7. Deviations from experimental data of vapor pressure calculated with the E-NRTL model with  
 407 OF-MV and parameters regressed in the region up to  $x_{\text{ion}} = 0.06$  and in the entire  $x_{\text{ion}}$  range for (water +  
 408 LiCl). References for the experimental datasets are provided in the Supporting Information.

#### 409 4 Data consistency analysis

410 This section presents results for the data consistency analysis. The impact of the objective  
 411 functions (Section 4.1) and the selection of water-salt parameters (Section 4.2) are discussed. Then,  
 412 the determination of the alcohol-salt parameters and the ternary results (Section 4.3) are shown.

#### 413 **4.1 Impact of the objective functions**

414 In this section, the impact of the objective functions are analyzed. OF-M, OF-V, and OF-MV  
415 are compared. In Table 2, the three objective functions are tested on (water + ethanol + NaCl). The  
416 resulting deviations on MIAC and VLE are evaluated. For OF-M, VLE results are predicted. For  
417 OF-V, MIAC results are predicted. The analysis is performed with two sets of water-salt parameters  
418 and different upper and lower bounds for the alcohol-salt parameters. Let us first focus on the 1st  
419 water-salt parameter set, which is the recommended set. The 2nd parameter set will be discussed  
420 in Section 4.2. Alcohol-salt parameters are optimized in two ranges  $[-5, -1)$ ,  $(4, 12]$  and  $[(4, 16),$   
421  $(4, 8)]$  (extended when boundaries are reached in optimizations), which are found to be reasonable  
422 ranges using a trial-and-error procedure.

423 One can observe that different optimal parameter sets could be found when different  
424 parameter ranges are imposed, indicating possible local minima in the OFs. In Table 2, results  
425 calculated with OF-M and OF-MV are approximately as good, only slightly better with the  
426 parameter set obtained in  $[-5, -1)$ ,  $(4, 12]$ . However, OF-V results in large deviations from the  
427 MIAC datasets, when parameters are regressed in both ranges. Therefore, in the cases that VLE is  
428 not available, VLE predictions are acceptable when using parameters regressed only based on  
429 MIAC; however, in the cases that MIAC is not available, MIAC predictions are likely to be far off  
430 when using parameters regressed only based on VLE.

431 Table 2. Alcohol-salt parameters regressed in different ranges and deviations of the E-NRTL model for (water + ethanol + NaCl) with two sets of water-salt  
 432 parameters (1st set:  $\tau_{sw} = -4.2915$ ,  $\tau_{ws} = 8.2464$ ; 2nd set:  $\tau_{sw} = -1.0391$ ,  $\tau_{ws} = -4.4583$ ). The information provided in the column on the left of the  
 433 parameter values are the ranges in which the parameters are regressed. AD stands for average deviation. MD stands for maximum deviation. Predicted values are  
 434 shown in italic and blue. Objective functions are as defined in Section 2.4.

	$\tau_{wa}$ & $\tau_{aw}$	OF	$\tau_{sa}$	$\tau_{as}$	$\alpha$	Esteso et al. <sup>70</sup>		Mamontov et al. <sup>71</sup>		Yang et al. <sup>46</sup> $p$		$y$		
						100AD	100MD	100AD	100MD	100AD	100MD	100AD	100MD	
1st	M	(- 5, - 1)	- 1.8983	(4, 12)	7.6887	0.2	2.4	7.2	0.91	2.7	<i>2.1</i>	<i>5.5</i>	<i>1.9</i>	<i>3.4</i>
		(4, 16)	15.978	(4, 8)	6.0436	0.2	2.5	7.4	1.1	3.7	<i>4.7</i>	<i>12</i>	<i>1.4</i>	<i>3.5</i>
	V	(- 5, 1)	- 0.12873	(4, 12)	5.3666	0.2	<i>3.9</i>	<i>8.8</i>	<i>3.9</i>	<i>8.8</i>	2.1	6.6	1.6	3.3
		(4, 16)	15.996	(4, 8)	4.3070	0.2	<i>5.9</i>	<i>19</i>	<i>7.5</i>	<i>21</i>	2.1	6.3	1.6	3.3
	MV	(- 5, - 1)	- 1.4847	(4, 12)	7.2184	0.2	2.4	7.2	0.91	2.9	2.2	6.5	1.6	3.3
		(4, 16)	16.000	(4, 8)	5.9058	0.2	2.5	7.4	1.2	3.0	4.5	11	1.4	3.3
2nd	M	(1, 5)	3.4910	(- 5, 1)	- 3.1604	0.2	3.3	8.9	1.6	4.2	<i>1.3</i>	<i>3.3</i>	<i>2.2</i>	<i>3.7</i>
	V	(1, 5)	3.2014	(- 5, 1)	- 1.3305	0.2	<i>3.3</i>	<i>8.9</i>	<i>1.7</i>	<i>4.3</i>	2.0	5.5	1.8	3.5
	MV	(1, 5)	3.5471	(- 5, 1)	- 1.8342	0.2	3.3	8.9	1.7	4.2	1.9	5.1	1.9	3.5

435



## 4.2 Selection of water-salt parameters

Modeling the aqueous electrolyte solutions is “simple”. Usually, a few sets of parameters result in approximately the same accuracy level. However, these parameters are not as good when extended to mixed-solvent electrolyte solutions. In Table 2, an example is provided for the (water + ethanol + NaCl) case. The optimal alcohol-salt parameters and ternary results calculated with the E-NRTL model and two sets of water-salt parameters are presented. The 1st water-salt parameter set is ( $\tau_{sw} = -4.2915$ ,  $\tau_{ws} = 8.2464$ ). The 2nd water-salt parameter set is ( $\tau_{sw} = -1.0391$ ,  $\tau_{ws} = -4.4583$ ). The 1st water-salt parameter set is regressed in a range that is close to the values reported by Chen’s group<sup>27,54</sup>. The 2nd parameter set is regressed in a different range. They are approximately as accurate for representing VLE and MIAC of the (water + NaCl) binary mixture. However, for the (water + ethanol + NaCl) ternary mixture, for both OF-M and OF-MV, the 2nd parameter set is less accurate for representing ternary MIAC, although approximately as accurate for the VLE dataset. Furthermore, the alcohol-salt parameter set is very different for the two water-salt parameter sets. Thus, the optimal parameters for the water-salt and alcohol-salt pairs are not independent. Therefore, in this work, parameters are regressed near the water-NaCl parameters as a first attempt for all the other water-salt pairs, which turns out to work very well.

## 4.3 Alcohol-salt parameters and ternary results

Table 3 shows the regressed parameters of the E-NRTL model for the (water + methanol/ethanol + alkali halide) mixtures. Parameters are regressed according to Eq. (9). Water-alcohol parameters are regressed to OF-V. Water-salt and alcohol-salt parameters are regressed to OF-M or OF-MV, depending on the data availability and reliability. The used (water + salt) datasets are summarized in the Supporting Information. Information of the used (water + alcohol + salt) datasets are summarized in Table 4. In many cases, reliable MIAC data are available at 298.15 K. Thus,  $\tau_{0,solvent-salt}$  and  $\tau_{0,salt-solvent}$  are first regressed; then, if reliable data are available at other temperatures, the temperature gradients,  $\tau_{1,solvent-salt}$  and  $\tau_{1,salt-solvent}$ , are regressed. When data are not available at 298.15 K, the  $\tau_0$  and  $\tau_1$  parameters are regressed together. The water-salt parameters are regressed to (water + salt) data, while the alcohol-salt parameters are regressed to (water + alcohol + salt) data. As we have shown in Section 4.1, OF-M and OF-MV can be used in parameter regression, while OF-V results in large deviations in MIAC predictions. For most of the listed mixtures, MIAC data are available. Solvent-salt parameters that are regressed to OF-M and

466 OF-MV are marked as bold in the table. In some cases, only VLE data are available; the solvent-  
467 salt parameters are regressed to OF-V, and are marked as green in the table. In a few cases for the  
468 mixed-solvent electrolyte mixtures, all the available datasets are decided to be unreliable after  
469 evaluation; the parameters are marked as blue and italic in the table. In some cases, data are only  
470 available at 298.15 K; no temperature gradient is given in the table. No trend is observed within  
471 the parameters. However, for all the water-salt pairs, the parameters are within a small range; for  
472 the alcohol-salt pairs, the parameters are more scattered, likely because of the lower consistency of  
473 the experimental datasets of the (water + alcohol + salt) ternary mixtures compared to those of the  
474 (water + salt) binary mixtures.

475 The overall average deviations (ADs) of the E-NRTL model from experimental datasets are  
476 presented in Table 5 along with results calculated using the other parameterization strategies. The  
477 ADs and maximum deviations (MDs) for each dataset are presented in the Supporting Information.  
478 Deviations are only shown for the mixtures for which the parameters that are regressed to OF-M  
479 and OF-MV. Temperature and composition ranges of the entire dataset are also shown. The datasets  
480 are only compared up to  $x_{\text{ion}} = 0.06$  and  $T = 400$  K. The behavior of the model beyond the  
481 composition range has been discussed in Section 3.3. The impact of temperature is captured by the  
482 temperature gradient introduced in Eq. (32), by the temperature dependence of the pure fluid  
483 density and relative permittivity, and by the temperature dependence in the model formulation. The  
484 two temperature gradient parameters do not present any trend, even though VLE data at different  
485 temperatures are included in the regressions. Parameter degeneracy is observed between the two  
486 temperature gradients. Figure 8 shows the comparison of MIAC calculated using the E-NRTL  
487 model and the experimental data for (water + ethanol + NaCl). The agreement between the  
488 experimental datasets from different sources, and between the datasets and the E-NRTL model,  
489 confirms the reliability of the evaluated experimental data, as well as that of the regressed  
490 parameters.

491 Table 3. Parameters of the E-NRTL model for the (water + methanol/ethanol + alkali halide) mixtures.  
 492 Water-alcohol parameters are regressed to OF-V. Water-salt and alcohol-salt parameters are regressed to  
 493 OF-M or OF-MV, depending on the data availability and reliability. The used (water + salt) datasets are  
 494 summarized in the Supporting Information. The relevant (water + alcohol + salt) datasets are summarized  
 495 in Table 4. Solvent-salt parameters that are regressed to OF-M and OF-MV are marked as bold.  
 496 Parameters that are determined based on unreliable (uncertain) datasets are marked as italic and blue.  
 497 Solvent-salt parameters that are regressed to OF-V are marked as green.

Binary pair ( <i>i-j</i> )	$\alpha$	A			
		$\tau_{0,ji}$	$\tau_{0,ij}$	$\tau_{1,ji}$	$\tau_{1,ij}$
Water-methanol	0.3	0.21334	0.29399	1175.2	- 1900.8
Water-ethanol	0.3	0.079833	1.4142	347.97	- 634.43
Solvent-salt parameters that are regressed to OF-M and OF-MV.					
<b>Water-LiCl</b>	<b>0.2</b>	<b>- 4.9031</b>	<b>9.3612</b>	<b>- 299.61</b>	<b>608.71</b>
<b>Water-NaCl</b>	<b>0.2</b>	<b>- 4.2915</b>	<b>8.2464</b>	<b>- 111.94</b>	<b>604.96</b>
<b>Water-KCl</b>	<b>0.2</b>	<b>- 4.0036</b>	<b>7.8180</b>	<b>- 550.87</b>	<b>1628.3</b>
<b>Water-RbCl</b>	<b>0.2</b>	<b>- 4.0639</b>	<b>8.0359</b>	<b>- 20.506</b>	<b>334.38</b>
<b>Water-CsCl</b>	<b>0.2</b>	<b>- 4.3330</b>	<b>8.7956</b>	<b>- 102.70</b>	<b>424.63</b>
<b>Water-NaF</b>	<b>0.2</b>	<b>- 4.5064</b>	<b>9.0168</b>	/	/
<b>Water-LiBr</b>	<b>0.2</b>	<b>- 5.0894</b>	<b>9.7570</b>	<b>685.09</b>	<b>- 2848.1</b>
<b>Water-NaBr</b>	<b>0.2</b>	<b>- 4.5219</b>	<b>8.6862</b>	<b>20.843</b>	<b>122.11</b>
<b>Water-KBr</b>	<b>0.2</b>	<b>- 4.0552</b>	<b>7.8781</b>	<b>332.36</b>	<b>- 998.97</b>
<b>Water-CsBr</b>	<b>0.2</b>	<b>- 4.2563</b>	<b>8.6560</b>	<b>53.154</b>	<b>- 212.31</b>
<b>Water-NaI</b>	<b>0.2</b>	<b>- 4.6495</b>	<b>8.8420</b>	<b>- 101.08</b>	<b>434.72</b>
<b>Water-KI</b>	<b>0.2</b>	<b>- 3.9659</b>	<b>7.5374</b>	<b>- 83.600</b>	<b>250.09</b>
<b>Methanol-LiCl</b>	<b>0.2</b>	<b>- 4.2412</b>	<b>9.0090</b>	<b>- 755.47</b>	<b>4409.9</b>
<b>Methanol-NaCl</b>	<b>0.2</b>	<b>- 2.4187</b>	<b>6.8712</b>	<b>563.09</b>	<b>1775.6</b>
<b>Methanol-KCl</b>	<b>0.2</b>	<b>- 2.6033</b>	<b>7.7412</b>	<b>- 1350.1</b>	<b>5212.9</b>
<b>Methanol-RbCl</b>	<b>0.2</b>	<b>- 2.8102</b>	<b>7.5196</b>	/	/
<b>Methanol-NaF</b>	<b>0.2</b>	<b>- 4.7905</b>	<b>15.000</b>	/	/
<b>Ethanol-NaCl</b>	<b>0.2</b>	<b>- 1.4847</b>	<b>7.2184</b>	<b>- 19.615</b>	<b>2077.0</b>
<b>Ethanol-KCl</b>	<b>0.2</b>	<b>- 0.10247</b>	<b>6.9013</b>	<b>2211.8</b>	<b>3698.4</b>
<b>Ethanol-CsCl</b>	<b>0.2</b>	<b>- 1.5844</b>	<b>7.4986</b>	/	/
<b>Ethanol-NaF</b>	<b>0.2</b>	<b>1.5302</b>	<b>14.980</b>	/	/
Parameters that are determined based on unreliable (uncertain) datasets.					
<i>Methanol-CsCl</i>	<i>0.2</i>	<i>- 3.3776</i>	<i>9.5764</i>	/	/

Binary pair ( <i>i-j</i> )	$\alpha$	A			
		$\tau_{0,ji}$	$\tau_{0,ij}$	$\tau_{1,ji}$	$\tau_{1,ij}$
<i>Methanol-NaBr</i>	0.2	-3.2938	6.8686	/	/
<i>Methanol-CsBr</i>	0.2	-4.8626	13.080	/	/
<i>Ethanol-LiCl</i>	0.2	-2.9328	7.9705	/	/
<i>Ethanol-NaBr</i>	0.2	-1.6454	6.4317	2788.69	-374.35
Solvent-salt parameters that are regressed to OF-V.					
<i>Ethanol-KBr</i>	0.2	-2.9567	6.0368	-646.38	642.01
<i>Ethanol-NaI</i>	0.2	-3.4167	7.0721	/	/
<i>Ethanol-KI</i>	0.2	-1.5412	1.9649	-703.52	-952.12

498 Table 4. Summary of the experimental datasets for the (water + methanol/ethanol + alkali halide)  
499 mixtures. The significance of the letters under “group” is explained in Section 5.2.

Reference	Group	$T$ (K)	$\text{Max}(x_{\text{ion}})$	$w_{\text{alc}}^0$	$N_{\text{DP}}$
<b>(water + methanol + LiCl)</b>					
<b>MIAC</b>					
Harned 1962 <sup>74</sup>	<b>T</b>	298.15	0.037	0.100 – 0.200	18
Mussini et al. 2000 <sup>45</sup>	<b>T</b>	298.15	0.131	0.200 – 0.800	128
Basili et al. 1999 <sup>75</sup>	<b>T</b>	298.15	0.131	0.200	12
Hu et al. 2008 <sup>76</sup>	<b>T</b>	298.15	0.027	0.050 – 0.150	46
<b>VLE</b>					
Broul et al. 1969 <sup>77</sup>	<b>T</b>	333.15	0.179	0.010 – 0.892	40
<b>(water + methanol + NaCl)</b>					
<b>MIAC</b>					
Xu et al. 2014 <sup>66</sup>	<b>R</b>	298.15	0.022	0.100	28
Basili et al. 1996 <sup>67</sup>	<b>R</b>	298.15	0.068	0.200 – 0.800	76
Yao et al. 1999 <sup>78</sup>	<b>R</b>	308.15 – 318.15	0.038	0.100 – 0.900	206
Hernandez-Hernandez et al. 2007 <sup>79</sup>	<b>R</b>	308.15	0.035	0.100	17
<b>VLE</b>					
Yang & Lee 1998 <sup>68</sup>	<b>R</b>	298.15	0.065	0.100 – 0.300	7
Yao et al. 1999 <sup>80</sup>	<b>R</b>	318.15	0.090	0.110 – 0.949	30
Johnson & Furter 1960 <sup>81</sup>	<b>R</b>	339.25 – 352.15	0.092	0.050 – 0.928	12
<b>(water + methanol + KCl)</b>					
<b>MIAC</b>					
Basili et al. 1997 <sup>69</sup>	<b>R</b>	298.15	0.037	0.200 – 0.600	47

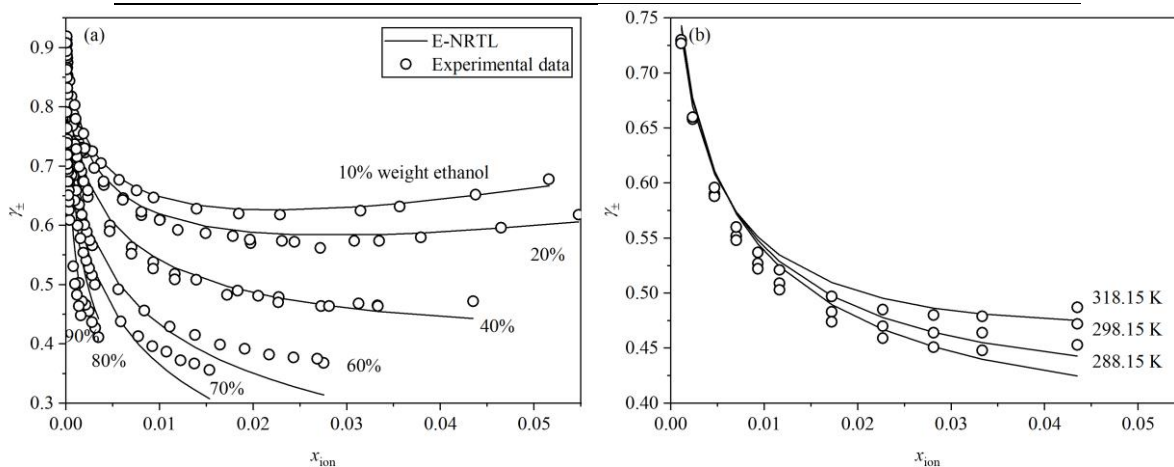
Reference	Group	$T$ (K)	$\text{Max}(x_{\text{ion}})$	$w_{\text{alc}}^0$	$N_{\text{DP}}$
Harned 1962 <sup>74</sup>	<b>T</b>	298.15	0.037	0.100 – 0.200	18
<b>VLE</b>					
Yang & Lee 1998 <sup>68</sup>	<b>R</b>	298.15	0.029	0.100 – 0.300	6
Johnson & Furter 1960 <sup>81</sup>	<b>R</b>	338.45 – 351.55	0.095	0.042 – 0.944	12
<b>(water + methanol + RbCl)</b>					
<b>MIAC</b>					
Zhang et al. 2004 <sup>82</sup>	<b>R</b>	298.15	0.043	0.100	9
Basili et al. 1997 <sup>69</sup>	<b>R</b>	298.15	0.068	0.200 – 0.800	67
<b>(water + methanol + CsCl)</b>					
<b>MIAC</b>					
Hu et al. 2007 <sup>83</sup>	<b>U</b>	298.15	0.029	0.100 – 0.400	72
Cui et al. 2007 <sup>84</sup>	<b>U</b>	298.15	0.061	0.100 – 0.400	64
Falciola et al. 2006 <sup>85</sup>	<b>U</b>	298.15	0.018	0.250 – 0.750	54
<b>(water + methanol + NaF)</b>					
<b>MIAC</b>					
Hernandez-Luis et al. 2003 <sup>86</sup>	<b>R</b>	298.15	0.010	0.100 – 0.900	113
<b>VLE</b>					
Boone et al. 1976 <sup>87</sup>	<b>U</b>	338.95 – 368.65	0.028	0.047 – 0.953	25
<b>(water + methanol + NaBr)</b>					
<b>MIAC</b>					
Han & Pan 1993 <sup>88</sup>	<b>U</b>	298.15	0.064	0.100 – 0.900	108
<b>VLE</b>					
Yang & Lee 1998 <sup>68</sup>	<b>T</b>	298.15	0.097	0.236 – 0.423	5
Boone et al. 1976 <sup>87</sup>	<b>U</b>	338.95 – 370.55	0.095	0.042 – 0.959	23
<b>(water + methanol + CsBr)</b>					
<b>MIAC</b>					
Falciola et al. 2006 <sup>85</sup>	<b>U</b>	298.15	0.018	0.250 – 0.750	54
<b>(water + methanol + CsI)</b>					
<b>MIAC</b>					
Falciola et al. 2006 <sup>85</sup>	<b>U</b>	298.15	0.018	0.250 – 0.750	54
<b>(water + ethanol + LiCl)</b>					
<b>MIAC</b>					
Hu et al. 2008 <sup>76</sup>	<b>U</b>	298.15	0.026	0.050 – 0.150	42

Reference	Group	$T$ (K)	$\text{Max}(x_{\text{ion}})$	$w_{\text{alc}}^0$	$N_{\text{DP}}$
Hernandez-Luis et al. 2008 <sup>89</sup> <b>VLE</b>	<b>U</b>	298.15	0.097	0.200 – 0.800	64
Shaw & Butler 1930 <sup>90</sup> <b>(water + ethanol + NaCl)</b> <b>MIAC</b>	<b>U</b>	298.15	0.133	0.148 – 0.992	24
Esteso et al. 1989 <sup>70</sup>	<b>R</b>	298.15	0.038	0.200 – 0.900	123
Mamontov et al. 2016 <sup>71</sup> <b>VLE</b>	<b>R</b>	288.15 – 318.15	0.055	0.100 – 0.400	117
Yang et al. 1979 <sup>46</sup>	<b>R</b>	298.15	0.025	0.100 – 0.700	22
Meyer et al. 1991 <sup>91</sup> <b>(water + ethanol + KCl)</b> <b>MIAC</b>	<b>T</b>	306.35 – 332.05	0.072	0.013 – 0.904	30
Mussini et al. 1995 <sup>72</sup> <b>VLE</b>	<b>R</b>	298.15	0.038	0.200 – 0.400	24
Yang et al. 1979 <sup>46</sup>	<b>R</b>	298.15	0.021	0.100 – 0.600	14
Sun 1996 <sup>92</sup> <b>(water + ethanol + CsCl)</b> <b>MIAC</b>	<b>R</b>	352.2 – 356.1	0.029	0.378 – 0.714	10
Mussini et al. 1995 <sup>72</sup> <b>(water + ethanol + NaF)</b> <b>MIAC</b>	<b>T</b>	298.15	0.112	0.200 – 0.700	59
Hernandez-Luis et al. 2003 <sup>86</sup> <b>(water + ethanol + LiBr)</b> <b>VLE</b>	<b>T</b>	298.15	0.011	0.100 – 0.800	89
Sun 1996 <sup>92</sup> <b>(water + ethanol + NaBr)</b> <b>MIAC</b>	<b>U</b>	352.51 – 356.07	0.050	0.378 – 0.714	12
Gonzalez-Diaz et al. 1995 <sup>93</sup>	<b>U</b>	298.15	0.027	0.200 – 0.998	100
Han & Pan 1993 <sup>88</sup> <b>VLE</b>	<b>U</b>	298.15	0.083	0.100 – 0.900	120
Sun 1996 <sup>92</sup> <b>(water + ethanol + KBr)</b> <b>VLE</b>	<b>U</b>	351.46 – 356.15	0.049	0.378 – 0.856	22

Reference	Group	$T$ (K)	$\text{Max}(x_{\text{ion}})$	$w_{\text{alc}}^0$	$N_{\text{DP}}$
Burns & Furter 1976 <sup>94</sup>	<b>T</b>	354.65 – 356.75	0.090	0.399 – 0.536	35
<b>(water + ethanol + CsBr)</b>					
<b>MIAC</b>					
Du et al. 2012 <sup>95</sup>	<b>U</b>	298.15	0.019	0.100 – 0.300	57
<b>(water + ethanol + NaI)</b>					
<b>VLE</b>					
Yamamoto et al. 1995 <sup>96</sup>	<b>T</b>	298.15	0.052	0.140 – 0.968	9
<b>(water + ethanol + KI)</b>					
<b>VLE</b>					
Sun 1996 <sup>92</sup>	<b>U</b>	351.63 – 356.05	0.038	0.533	15
Burns & Furter 1979 <sup>97</sup>	<b>T</b>	355.25 – 357.15	0.106	0.384 – 0.856	21

500 Table 5. Overall ADs of the E-NRTL model from the experimental datasets

	100ADs	
	(water + methanol + salt) mixtures	(water + ethanol + salt) mixtures
MIAC	1.3	1.9
VLE, $p$	2.0	2.4
$y$	0.86	1.7



501  
502 Figure 8. Comparison of MIAC calculated using the E-NRTL model and the experimental data <sup>70,71</sup> for  
503 (water + ethanol + NaCl): (a) 298.15 K at different ethanol compositions, (b) 40% weight fraction (salt-  
504 free basis) of ethanol at different temperatures

## 505 5 Benchmark database

506 In this section, the benchmark databases of the aqueous and mixed-solvent electrolyte  
507 solutions are presented.

## 508 **5.1 Database for aqueous electrolyte solutions**

509 Compared to the data status of the mixed-solvent electrolyte solutions, that of the aqueous  
510 electrolyte binary mixtures is much more extensive, which facilitates selection of the datasets that  
511 are validated in higher accuracy. Thus, only the selected datasets are shown here. The accepted  
512 MIAC and VLE datasets of the (water + salt) mixtures are summarized in the Supporting  
513 Information. The maximum  $x_{\text{ion}}$  column in the summary table shows the maximum value in the  
514 entire dataset. However, only the part that is smaller than  $x_{\text{ion}} = 0.06$  is used in the regression and  
515 comparison, because the E-NRTL model deviates significantly from experimental values at large  
516 salt composition, as discussed in Section 3.3.

## 517 **5.2 Database for mixed-solvent electrolyte solutions**

518 The MIAC and VLE datasets of the (water + alcohol + salt) mixed-solvent electrolyte  
519 solutions are summarized in Table 4. Compared to the data status of the aqueous electrolyte  
520 solutions, that of the mixed-solvent electrolyte solutions is much less extensive. In some cases,  
521 there is only one dataset, or there are datasets that are contradictory to each other, so that they  
522 cannot be verified. Therefore, datasets are marked as “**R**” (recommended), “**T**” (tentative), and “**U**”  
523 (unknown). Group **R** denotes datasets that have been verified against other datasets with deviations  
524 within a few percent, e.g., the datasets of (water + methanol + NaCl). In many cases, such  
525 verifications are not possible, because data are scarce or contradictory between different sources.  
526 In these cases, when there is only one dataset for the mixture, group **T** denotes datasets that are  
527 considered reliable by us, based on data trends and ranges, while group **U** denotes datasets that are  
528 considered unreliable by us. When there are multiple datasets available for the mixture, group **T**  
529 denotes datasets that deviate from each other but not by too much, while group **U** denotes datasets  
530 that deviate from each other by a lot so that it is not possible to decide which one or ones are  
531 reliable. As discussed in Section 2.1, experimental literature does not report the combined  
532 uncertainty of MIAC. For group **R** datasets, data from different sources agree with each other  
533 within a few percent; in most cases, one can expect the data to be very accurate. For group **T**  
534 datasets, discrepancy between data of different sources exceed 10% at boundaries of data ranges.  
535 For group **U** datasets, as no comparison can be made between data of different sources, accuracy  
536 cannot be estimated. The data tables are provided in the Supporting Information. Group **R** and **T**  
537 datasets are provided in the same file, while group **U** datasets are provided in a separate file. For



538 datasets that are marked as **T** and **U**, reasons are given in the following text in this section. These  
539 explanations are to be read together with the dataset summary in Table 4.

540 For (water + methanol + LiCl), although there are a few datasets, they do not agree with each  
541 other. The Hu et al. dataset <sup>76</sup> is smaller than the Harned dataset <sup>74</sup> by a few percent, while the  
542 datasets from the Mussini group <sup>45,75</sup> is larger by a few percent. A maximum deviation that is  
543 approximately 10% is observed in the only VLE dataset <sup>77</sup> as it is regressed along with the MIAC  
544 datasets. Therefore, these datasets are all marked as **T**. For this mixture, there is another MIAC  
545 dataset <sup>98</sup>, which also covers a few other mixtures in Table 4. However, it is rejected because that  
546 scattering is up to a few percent within their own datasets for a few mixtures, and that these datasets  
547 do not agree with the **R** datasets that are available for some of these mixtures. There is another  
548 VLE dataset <sup>87</sup>. However, after regression, large deviations are observed for vapor phase molar  
549 fraction, which indicates that it is not reliable. Furthermore, datasets from the same reference are  
550 found to deviate significantly from the **R** datasets of a few other mixtures. Therefore, they are not  
551 included in the table.

552 For (water + methanol + NaCl), apart from the datasets summarized in Table 4, there are a  
553 few other datasets for MIAC and VLE <sup>74,98-102</sup>. However, the **R** datasets agree very well with each  
554 other. Therefore, these datasets are not included in the table. For MIAC, datasets from references  
555 <sup>98,99</sup> deviate significantly from the **R** datasets, while datasets from references <sup>74,100,101</sup> deviate from  
556 the **R** datasets by only a few percent. For VLE, there is another dataset <sup>102</sup>. However, the vapor  
557 phase molar fraction deviates significantly from the **R** datasets.

558 For (water + methanol + KCl), the Harned <sup>74</sup> dataset is marked as **T** because the Basili et al.  
559 <sup>69</sup> dataset agrees very well when regressed together with the VLE datasets <sup>68,81</sup>, while it deviates by  
560 a few percent. Because the Basili et al. <sup>69</sup> MIAC dataset covers larger composition range, the  
561 Harned <sup>74</sup> dataset is not included in parameter regression. There are another MIAC dataset <sup>98</sup> and  
562 another VLE dataset <sup>87</sup>. However, they are not included in this table because they deviate from the  
563 **R** and **T** datasets significantly.

564 For (water + methanol + CsCl), the three available MIAC datasets <sup>83-85</sup> deviate significantly  
565 from each other. Therefore, no conclusion can be drawn and they are marked as **U**.

566 For (water + methanol + NaF), the Boone et al. VLE dataset<sup>87</sup> is marked as **U** because that it  
567 cannot be regressed to an accuracy within 10% even though NaF has a very low salt solubility, and  
568 that datasets from the same reference are found to deviate significantly from the **R** datasets of a  
569 few other mixtures.

570 For (water + methanol + NaBr), the MIAC dataset<sup>88</sup> and Boone et al. VLE dataset<sup>87</sup> are  
571 marked as **U**, because they deviate significantly when regressed together. Plotted on the graph (as  
572 shown in the Supporting Information), the MIAC data are clustered unreasonably: 40% ethanol  
573 weight fraction (salt-free basis) data are clustered with 60% data; while large gaps are present  
574 between the 20% and 40% data, and between the 60% and 80% data. Such behavior is not  
575 successfully correlated with the E-NRTL model. Thus, verifications against the **U** MIAC datasets  
576 cannot conclude on the reliability of the Yang and Lee VLE dataset<sup>68</sup>. However, datasets from the  
577 same reference have been verified for other mixtures. In addition, it is represented well with the E-  
578 NRTL model. Furthermore, the Yang and Lee dataset only covers small alcohol composition, and  
579 thus can be considered to be verified against the accepted (water + NaBr) datasets. Therefore, it is  
580 marked as **T**.

581 For (water + methanol + CsI), the Falciola et al.<sup>85</sup> dataset is the only available dataset, and  
582 thus cannot be verified. In addition, the Falciola et al. dataset present a strange behavior at high  
583 alcohol composition (75% weight fraction on the salt-free basis): at 0.018 ion-based molar fraction  
584 (approximately 0.5 M), MIAC increases to as large as 5. Such behavior is not observed in the (water  
585 + methanol + CsCl) and (water + methanol + CsBr) datasets and the lower-alcohol-composition  
586 part of the (water + methanol + CsI) dataset from the same reference, and cannot be represented  
587 with the E-NRTL model. Therefore, it is marked as **U**.

588 For (water + methanol + CsBr), the Falciola et al.<sup>85</sup> dataset is also marked as **U**. There is  
589 another dataset for this mixture by Du et al.<sup>95</sup>. However, MIAC decreases to very small values in  
590 the Du et al.<sup>95</sup> dataset. Such behavior is not observed in any of the **R** and **T** datasets of the  
591 investigated mixtures. Therefore, it is not included in Table 4.

592 For (water + ethanol + LiCl), the two MIAC datasets<sup>76,89</sup> and the VLE dataset<sup>90</sup> do not agree  
593 with each other. The 5%-15% ethanol weight fraction (salt-free basis) data from the Hu et al.<sup>76</sup>  
594 dataset is smaller than the 20% data from the Hernandez-Luis dataset<sup>89</sup>, which is against the overall

595 trend that MIAC is smaller for the data at larger alcohol composition. Regression with the two  
596 MIAC datasets together with the VLE dataset does not result in any preference between them. In  
597 addition, there are two other VLE datasets <sup>92,103</sup>. However, they present vapor phase molar fraction  
598 that deviates significantly after regression, which is very unlikely for reliable data. Therefore, they  
599 are not included in the table. A dataset from reference <sup>103</sup> is also rejected after comparison with the  
600 recommended datasets for (water + ethanol + NaCl). However, datasets from reference <sup>92</sup> agrees  
601 well with the other **R** datasets for (water + ethanol + KCl) (marked as **R**), (water + ethanol + KI)  
602 (marked as **R**), and (water + ethanol + NaBr) (marked as **T** because the quality of other datasets of  
603 this mixture is not as good as that of the KCl and KI mixtures). In the meantime, being the only  
604 dataset for (water + ethanol + LiBr), a dataset from the same reference cannot be represented  
605 accurately after regression, and is marked as **U**.

606 For (water + ethanol + NaCl), in addition to the VLE dataset from reference <sup>103</sup>, there is an  
607 additional MIAC dataset <sup>104</sup> that is not included in Table 4, because it deviates significantly from  
608 the **R** datasets. The Meyer et al. <sup>91</sup> dataset is marked as **T**, because its vapor phase molar fraction  
609 deviation is slightly larger than 10% after regression, while the other datasets agree very well with  
610 the model. Despite this, it is included in the table because it is the only VLE dataset at temperatures  
611 other than 298.15 K.

612 For (water + ethanol + CsCl), the Mussini et al. <sup>72</sup> dataset is marked as **T**. It is represented  
613 very well with the E-NRTL model. There is another MIAC dataset for this mixture by Hu et al. <sup>83</sup>.  
614 However, the data decreases to very small values at smaller than 0.008 ion-based molar fraction.  
615 Such behavior is not observed in any other investigated mixtures. A dataset from reference <sup>83</sup> is  
616 among the three MIAC datasets of (water + methanol + CsCl) that are contradictory to each other.  
617 In addition, a dataset from the same reference is rejected in the evaluation for the (water + CsCl)  
618 datasets, although not because of wrong trend, but rather only because of relatively larger  
619 deviations compared to the accepted datasets. Therefore, the Hu et al. <sup>83</sup> dataset is not included in  
620 Table 4.

621 For (water + ethanol + NaF), the Hernandez-Luis et al. dataset <sup>86</sup> is the only available dataset.  
622 Although it is not verified against other datasets, it is unlikely to be far off because of the very  
623 small solubility of NaF. In addition, it is very well represented with the E-NRTL model. Therefore,  
624 it is marked as **T**.

625 For (water + ethanol + NaBr), in the same range as the Gonzalez-Dias et al. dataset <sup>93</sup>, the Han  
626 and Pan dataset <sup>88</sup> is slightly smaller. Furthermore, at larger salt composition, the upward curvature  
627 that seems quite artificial cannot be represented with the E-NRTL model. There is no dataset to  
628 verify the Han and Pan dataset, considering that the only VLE dataset is from a reference <sup>92</sup> in  
629 which datasets have been evaluated to be unreliable for a few other mixtures. In addition, a dataset  
630 is marked as **U** from the reference <sup>88</sup> for (water + methanol + NaBr). Therefore, the VLE dataset  
631 are marked as **T**, while the MIAC datasets are both marked as **U**. However, because no dataset of  
632 better quality is available, all three datasets have been used in the regression.

633 For (water + ethanol + KBr) and (water + ethanol + NaI), each mixture only has one VLE  
634 dataset <sup>94,96</sup>. Thus, they are not verified, but are represented very well with the E-NRTL model.  
635 Therefore, they are marked as **T**.

636 For (water + ethanol + CsBr), the only dataset is from reference <sup>95</sup>. It has the same problem as  
637 the (water + methanol + CsBr) from the same reference, presenting very small MIAC values that  
638 are not observed in any of the **R** and **T** datasets in the investigated mixtures. Therefore, it is marked  
639 as **U**.

640 For (water + ethanol + KI), there is another VLE dataset <sup>105</sup> that deviates significantly from  
641 the **T** dataset. It is not included in Table 4. The Sun <sup>92</sup> dataset deviates more compared to the **T**  
642 dataset after regression. Considering that datasets from the same reference also present larger  
643 deviations compared to the **R** datasets of other mixtures when more detailed comparisons are  
644 possible, the Sun <sup>92</sup> dataset is marked **U**. Therefore, the remaining VLE dataset cannot be verified,  
645 and is marked as **T**.

646 Figure 9 shows the data status of the (water + methanol/ethanol + alkali halide) ternary  
647 mixtures. As the datasets are evaluated, 13 of the 20 mixtures for which experimental data are  
648 available can be confirmed against data from other sources. From the perspectives of data quality  
649 and availability, we recommend that further experimental work be conducted on mixtures that only  
650 have **U** datasets (red), and on mixtures that have not been measured yet (white).

(a)

	F <sup>-</sup>	Cl <sup>-</sup>	Br <sup>-</sup>	I <sup>-</sup>
Li <sup>+</sup>				
Na <sup>+</sup>				
K <sup>+</sup>				
Rb <sup>+</sup>				
Cs <sup>+</sup>				

(b)

	F <sup>-</sup>	Cl <sup>-</sup>	Br <sup>-</sup>	I <sup>-</sup>
Li <sup>+</sup>				
Na <sup>+</sup>				
K <sup>+</sup>				
Rb <sup>+</sup>				
Cs <sup>+</sup>				

651

652 Figure 9. Data status of the ternary mixtures: (a) (water + methanol + alkali halide), (b) (water + ethanol +  
 653 alkali halide). The green color denotes that there are **R** data for both MIAC and VLE. The light green  
 654 color denotes that there are **R** data for MIAC only. The blue color denotes that there are **T** data for MIAC.  
 655 The orange color denotes that there are **R** or **T** data for VLE only. The red color denotes that all available  
 656 data are marked as **U**. The white color denotes that there are no data.

## 657 **6 Conclusions and perspectives**

658 In this work, a benchmark database for (water + methanol/ethanol + alkali halide) mixed-  
 659 solvent electrolyte solutions is presented. A consistent E-NRTL model that satisfies the Gibbs-  
 660 Duhem equation is utilized for data analysis, reconciling solvent and ion composition derivatives  
 661 of the excess Gibbs energy, and thus reconciling MIAC and VLE. Major conclusions are:

- 662 1. Available experimental data of MIAC and VLE are comprehensively collected and critically  
 663 evaluated for the 61 datasets of 20 solutions. The resulting benchmark database covers 1413  
 664 data records from 32 datasets for 13 solutions. Evaluated datasets that are used in the  
 665 parameterization of the relevant water-salt pair are also presented.

666 2. The consistent E-NRTL model is compared against the widely used original E-NRTL model.  
667 Results and parameters indicate that the consistent model better reconciles MIAC and VLE,  
668 especially the salting out effect of the co-solvent (alcohol) when it is highly diluted in water.

669 3. A consistency analysis is conducted within each solution. Impacts of the objective functions  
670 and water-salt parameters are discussed, facilitating the parameterization and data analysis.  
671 Recommended parameters are obtained based on the obtained benchmark database.

672 Considering that alcohol and monovalent strong salts represent the simplest components in  
673 mixed-solvent electrolyte solutions, we propose that the database be used as a benchmark for model  
674 development and evaluation, as thermodynamic property models are extended to mixed-solvent  
675 electrolyte solutions.

## 676 **Nomenclature**

677  $A_\phi$  One third of the Debye-Huckel limiting slope

678 AD Average deviation

679 E-NRTL Electrolyte non-random two-liquid

680  $G^E$  Excess Gibbs energy

681  $I_x$  Ionic strength

682  $k$  Boltzmann constant

683  $m$  Molality

684  $M$  Molar mass

685 MD Maximum deviation

686 MIAC Mean ionic activity coefficient

687  $n$  Molar amount

688  $N_A$  Avogadro number

689	OF	Objective function
690	OF-M	OF = MIAC
691	OF-MV	OF = MIAC + VLE
692	OF-V	OF = VLE
693	$p$	Pressure
694	PDH	Pitzer-Debye-Huckel
695	$Q_e$	Elementary charge
696	$r$	Born radius
697		Pauling radius
698	$R$	Universal gas constant
699	<b>R</b>	Recommended datasets
700	SLE	Solid-liquid equilibrium
701	$T$	Temperature
702	<b>T</b>	Tentative datasets
703	<b>U</b>	Uncertain datasets
704	VLE	Vapor-liquid equilibrium
705	$w^0$	Weight fraction on the salt-free basis
706	$x$	Molar fraction (in general or in the liquid phase)
707	$x^0$	Composition in the original unit
708		Molar fraction on the salt-free basis
709	$y$	Molar fraction in the vapor phase

710	$Z$	Ionic charge
711	<b>Greek letters</b>	
712	$\alpha$	Parameter in the NRTL term
713	$\gamma$	Activity coefficient
714	$\Delta g_{\text{trans}}$	Molar Gibbs energy of transfer
715	$\Delta_f g$	Standard Gibbs energy of formation
716	$\Delta p$	Vapor pressure depression
717	$\varepsilon$	Relative permittivity
718	$\varepsilon_0$	Dielectric constant in the vacuum
719	$\nu$	Stoichiometric coefficient
720	$\rho$	Density
721	$\tau$	Parameter in the NRTL term
722	<b>Subscript</b>	
723	$\pm$	Mean ionic
724	a	Anion
725	(a)	Reference state at infinite dilution in water
726	c	Cation
727	m	Molecule
728	s	Solvent mixture
729	(s)	Solid phase
730	w	Water



731 **Superscript**

732	*	Rational unsymmetrical
733	$\infty$	Infinite dilution
734	m	Molality
735	c	Molarity
736	sat	Saturation state of pure solvent

737 **Supporting Information**

738 Supporting Information are provided for the following contents:

- 739 - Analytical expressions for  $\left(\frac{\partial A_\phi}{\partial n_i}\right)_{T,p,n_{j(j\neq i)}}$  and the other derivatives over  $n_i$ .
- 740 - Solvent activity coefficients of (water + methanol + KCl) and (water + ethanol +  
741 NaCl/KCl).
- 742 - Parameters for solvent component density and relative permittivity.
- 743 - Parameters of the consistent and original E-NRTL models for (water + methanol/ethanol  
744 + NaCl/KCl) with OF-M and OF-MV.
- 745 - Deviations of MIAC calculated with the E-NRTL model with OF-MV and parameters  
746 regressed in the region up to  $x_{\text{ion}} = 0.06$  and in the entire  $x_{\text{ion}}$  range.
- 747 - Average and maximum deviations of the e-NRTL model from the experimental datasets.
- 748 - Summary of accepted MIAC and VLE datasets for aqueous electrolyte solutions.
- 749 - Benchmark database files for the mixed-solvent electrolyte solutions and relevant  
750 aqueous electrolyte solutions.
- 751 - MIAC results for the mixed-solvent electrolyte solutions.

752 The information is available free of charge via the Internet at <http://pubs.acs.org/>.

## 753 **Notes**

754 The authors declare no competing financial interest.

## 755 **Acknowledgement**

756 The authors wish to thank the European Research Council (ERC) for funding of this research  
757 under European Union's Horizon 2020 research and innovation program (grant agreement No.  
758 832460), ERC Advanced Grant project "New Paradigm in Electrolyte Thermodynamics".

## 759 **Reference:**

- 760 (1) Bui, M.; Adjiman, C. S.; Bardow, A.; Anthony, E. J.; Boston, A.; Brown, S.; Fennell, P.  
761 S.; Fuss, S.; Galindo, A.; Hackett, L. A.; Hallett, J. P.; Herzog, H. J.; Jackson, G.; Kemper,  
762 J.; Krevor, S.; Maitland, G. C.; Matuszewski, M.; Metcalfe, I. S.; Petit, C.; Puxty, G.;  
763 Reimer, J.; Reiner, D. M.; Rubin, E. S.; Scott, S. A.; Shah, N.; Smit, B.; Trusler, J. P. M.;  
764 Webley, P.; Wilcox, J.; Mac Dowell, N. Carbon Capture and Storage (CCS): The Way  
765 Forward. *Energy Environ. Sci.* **2018**, *11* (5), 1062–1176.  
766 <https://doi.org/10.1039/c7ee02342a>.
- 767 (2) Gholami, F.; Tomas, M.; Gholami, Z.; Vakili, M. Technologies for the Nitrogen Oxides  
768 Reduction from Flue Gas: A Review. *Sci. Total Environ.* **2020**, *714*, 136712.  
769 <https://doi.org/10.1016/j.scitotenv.2020.136712>.
- 770 (3) Darre, N. C.; Toor, G. S. Desalination of Water: A Review. *Curr. Pollut. Reports* **2018**, *4*  
771 (2), 104–111. <https://doi.org/10.1007/s40726-018-0085-9>.
- 772 (4) Løge, I. A.; Bentzon, J. R.; Klingaa, C. G.; Walther, J. H.; Anabaraonye, B. U.; Fosbøl, P.  
773 L. Scale Attachment and Detachment: The Role of Hydrodynamics and Surface  
774 Morphology. *Chem. Eng. J.* **2021**, *430* (P2), 132583.  
775 <https://doi.org/10.1016/j.cej.2021.132583>.
- 776 (5) Olasunkanmi, L. O. Corrosion: Favoured, yet Undesirable - Its Kinetics and  
777 Thermodynamics. In *Corrosion*; IntechOpen: London, 2021; pp 1–17.
- 778 (6) Yu, Z.; Wang, H.; Kong, X.; Huang, W.; Tsao, Y.; Mackanic, D. G.; Wang, K.; Wang, X.;  
779 Huang, W.; Choudhury, S.; Zheng, Y.; Amanchukwu, C. V.; Hung, S. T.; Ma, Y.; Lomeli,  
780 E. G.; Qin, J.; Cui, Y.; Bao, Z. Molecular Design for Electrolyte Solvents Enabling  
781 Energy-Dense and Long-Cycling Lithium Metal Batteries. *Nat. Energy* **2020**, *5* (7), 526–

- 782 533. <https://doi.org/10.1038/s41560-020-0634-5>.
- 783 (7) Molla, G. S.; Freitag, M. F.; Stocks, S. M.; Nielsen, K. T.; Sin, G. Solubility Prediction of  
784 Different Forms of Pharmaceuticals in Single and Mixed Solvents Using Symmetric  
785 Electrolyte Nonrandom Two-Liquid Segment Activity Coefficient Model. *Ind. Eng. Chem.*  
786 *Res.* **2019**, *58* (10), 4267–4276. <https://doi.org/10.1021/acs.iecr.8b04268>.
- 787 (8) Bazyleva, A.; Abildskov, J.; Anderko, A.; Baudouin, O.; Chernyak, Y.; de Hemptinne, J.  
788 C.; Diky, V.; Dohrn, R.; Elliott, J. R.; Jacquemin, J.; Jaubert, J. N.; Joback, K. G.; Kattner,  
789 U. R.; Kontogeorgis, G. M.; Loria, H.; Mathias, P. M.; O’Connell, J. P.; Schröer, W.;  
790 Smith, G. J.; Soto, A.; Wang, S.; Weir, R. D. Good Reporting Practice for Thermophysical  
791 and Thermochemical Property Measurements (IUPAC Technical Report). *Pure Appl.*  
792 *Chem.* **2021**, *93* (2), 253–272. <https://doi.org/10.1515/pac-2020-0403>.
- 793 (9) May, P. M.; Rowland, D. Correction to Thermodynamic Modeling of Aqueous Electrolyte  
794 Systems: Current Status (Journal of Chemical & Engineering Data (2017) 62:9 (2481-  
795 2495) DOI: 10.1021/Acs.Jced.6b01055). *J. Chem. Eng. Data* **2019**, *64* (7), 3212.  
796 <https://doi.org/10.1021/acs.jced.9b00468>.
- 797 (10) Kontogeorgis, G. M.; Dohrn, R.; Economou, I. G.; De Hemptinne, J. C.; Kate, A.;  
798 Kuitunen, S.; Mooijer, M.; Zilnik, L. F.; Vesovic, V. Industrial Requirements for  
799 Thermodynamic and Transport Properties: 2020. *Ind. Eng. Chem. Res.* **2021**, *60* (13),  
800 4987–5013. <https://doi.org/10.1021/acs.iecr.0c05356>.
- 801 (11) Kontogeorgis, G. M.; Maribo-Mogensen, B.; Thomsen, K. The Debye-Hückel Theory and  
802 Its Importance in Modeling Electrolyte Solutions. *Fluid Phase Equilib.* **2018**, *462*, 130–  
803 152. <https://doi.org/10.1016/j.fluid.2018.01.004>.
- 804 (12) Simonin, J. P. On the “Born” Term Used in Thermodynamic Models for Electrolytes. *J.*  
805 *Chem. Phys.* **2019**, *150*, 244503. <https://doi.org/10.1063/1.5096598>.
- 806 (13) Thomsen, K. *Electrolyte Solutions: Thermodynamics, Crystallization, Separation*  
807 *Methods*; Technical University of Denmark: Kgs. Lyngby, 2009.  
808 <https://doi.org/10.11581/dtu:00000073>.
- 809 (14) Vaque Aura, S.; Roa Pinto, J. S.; Ferrando, N.; De Hemptinne, J. C.; Ten Kate, A.;  
810 Kuitunen, S.; Diamantonis, N.; Gerlach, T.; Heilig, M.; Becker, G.; Brehelin, M. Data  
811 Analysis for Electrolyte Systems: A Method Illustrated on Alkali Halides in Water. *J.*  
812 *Chem. Eng. Data* **2021**, *66* (8), 2976–2990. <https://doi.org/10.1021/acs.jced.1c00105>.

- 813 (15) Raatschen, W.; Harvey, A. H.; Prausnitz, J. M. Equation of State for Solutions of  
814 Electrolytes in Mixed Solvents. *Fluid Phase Equilib.* **1987**, *38* (1–2), 19–38.  
815 [https://doi.org/10.1016/0378-3812\(87\)90002-1](https://doi.org/10.1016/0378-3812(87)90002-1).
- 816 (16) Zuo, Y. X.; Fürst, W. Use of an Electrolyte Equation of State for the Calculation of Vapor-  
817 Liquid Equilibria and Mean Activity Coefficients in Mixed Solvent Electrolyte Systems.  
818 *Fluid Phase Equilib.* **1998**, *150* (151), 267–275. [https://doi.org/10.1016/s0378-](https://doi.org/10.1016/s0378-3812(98)00326-4)  
819 [3812\(98\)00326-4](https://doi.org/10.1016/s0378-3812(98)00326-4).
- 820 (17) Simon, H. G.; Kistenmacher, H.; Prausnitz, J. M.; Vortmeyer, D. An Equation of State for  
821 Systems Containing Electrolytes and Nonelectrolytes. *Chem. Eng. Process.* **1991**, *29* (3),  
822 139–146. [https://doi.org/10.1016/0255-2701\(91\)85013-E](https://doi.org/10.1016/0255-2701(91)85013-E).
- 823 (18) Zuo, J. Y.; Zhang, D.; Fürst, W. Predicting LLE in Mixed-Solvent Electrolyte Systems by  
824 an Electrolyte EOS. *AIChE J.* **2000**, *46* (11), 2318–2329.  
825 <https://doi.org/10.1002/aic.690461122>.
- 826 (19) Zuo, J. Y.; Zhang, D.; Fürst, W. Extension of the Electrolyte EOS of Furst and Renon to  
827 Mixed Solvent Electrolyte Systems. *Fluid Phase Equilib.* **2000**, *175* (1–2), 285–310.  
828 [https://doi.org/10.1016/S0378-3812\(00\)00463-5](https://doi.org/10.1016/S0378-3812(00)00463-5).
- 829 (20) Held, C.; Reschke, T.; Mohammad, S.; Luza, A.; Sadowski, G. EPC-SAFT Revised.  
830 *Chem. Eng. Res. Des.* **2014**, *92* (12), 2884–2897.  
831 <https://doi.org/10.1016/j.cherd.2014.05.017>.
- 832 (21) Schreckenber, J. M. A.; Dufal, S.; Haslam, A. J.; Adjiman, C. S.; Jackson, G.; Galindo,  
833 A. Modelling of the Thermodynamic and Solvation Properties of Electrolyte Solutions  
834 with the Statistical Associating Fluid Theory for Potentials of Variable Range. *Mol. Phys.*  
835 **2014**, *112* (17), 2339–2364. <https://doi.org/10.1080/00268976.2014.910316>.
- 836 (22) Maribo-Mogensen, B.; Thomsen, K.; Kontogeorgis, G. M. An Electrolyte CPA Equation  
837 of State for Mixed Solvent Electrolytes. *AIChE J.* **2015**, *61* (9), 2933–2950.  
838 <https://doi.org/10.1002/aic.14829>.
- 839 (23) Das, G.; dos Ramos, M. C.; McCabe, C. Predicting the Thermodynamic Properties of  
840 Experimental Mixed-Solvent Electrolyte Systems Using the SAFT-VR+DE Equation of  
841 State. *Fluid Phase Equilib.* **2018**, *460*, 105–118.  
842 <https://doi.org/10.1016/j.fluid.2017.11.017>.
- 843 (24) Ahmed, S.; Ferrando, N.; de Hemptinne, J. C.; Simonin, J. P.; Bernard, O.; Baudouin, O.

- 844 Modeling of Mixed-Solvent Electrolyte Systems. *Fluid Phase Equilib.* **2018**, *459*, 138–  
845 157. <https://doi.org/10.1016/j.fluid.2017.12.002>.
- 846 (25) Neau, E.; Nicolas, C.; Avaullée, L. Extension of the Group Contribution NRTL-PRA EoS  
847 for the Modeling of Mixtures Containing Light Gases and Alcohols with Water and Salts.  
848 *Fluid Phase Equilib.* **2018**, *458*, 194–210. <https://doi.org/10.1016/j.fluid.2017.09.028>.
- 849 (26) Mock, B.; Evans, L. B.; Chen, C. -C. Thermodynamic Representation of Phase Equilibria  
850 of Mixed-solvent Electrolyte Systems. *AIChE J.* **1986**, *32* (10), 1655–1664.  
851 <https://doi.org/10.1002/aic.690321009>.
- 852 (27) Chen, C. C.; Song, Y. Generalized Electrolyte-NRTL Model for Mixed-Solvent  
853 Electrolyte Systems. *AIChE J.* **2004**, *50* (8), 1928–1941. <https://doi.org/10.1002/aic.10151>.
- 854 (28) Macedo, E. A.; Skovborg, P.; Rasmussen, P. Calculation of Phase Equilibria for Solutions  
855 of Strong Electrolytes in Solvent-Water Mixtures. *Chem. Eng. Sci.* **1990**, *45* (4), 875–882.  
856 [https://doi.org/10.1016/0009-2509\(90\)85009-3](https://doi.org/10.1016/0009-2509(90)85009-3).
- 857 (29) Sander, B.; Fredenslund, A.; Rasmussen, P. Calculation of Vapour-Liquid Equilibria in  
858 Mixed Solvent/Salt Systems Using an Extended UNIQUAC Equation. *Chem. Eng. Sci.*  
859 **1986**, *41* (5), 1171–1183. [https://doi.org/10.1016/0009-2509\(86\)87090-7](https://doi.org/10.1016/0009-2509(86)87090-7).
- 860 (30) Zerres, H.; Prausnitz, J. M. Thermodynamics of Phase Equilibria in Aqueous-organic  
861 Systems with Salt. *AIChE J.* **1994**, *40* (4), 676–691.  
862 <https://doi.org/10.1002/aic.690400411>.
- 863 (31) Van Bochove, G. H.; Krooshof, G. J. P.; De Loos, T. W. Modelling of Liquid-Liquid  
864 Equilibria of Mixed Solvent Electrolyte Systems Using the Extended Electrolyte NRTL.  
865 *Fluid Phase Equilib.* **2000**, *171* (1–2), 45–58. [https://doi.org/10.1016/S0378-](https://doi.org/10.1016/S0378-3812(00)00347-2)  
866 [3812\(00\)00347-2](https://doi.org/10.1016/S0378-3812(00)00347-2).
- 867 (32) Thomsen, K. Modeling Electrolyte Solutions with the Extended Universal Quasichemical  
868 (UNIQUAC) Model. *Pure Appl. Chem.* **2005**, *77* (3), 531–542.  
869 <https://doi.org/10.1351/pac200577030531>.
- 870 (33) Djamali, E.; Kan, A. T.; Tomson, M. B. A Priori Prediction of Thermodynamic Properties  
871 of Electrolytes in Mixed Aqueous-Organic Solvents to Extreme Temperatures. *J. Phys.*  
872 *Chem. B* **2012**, *116* (30), 9033–9042. <https://doi.org/10.1021/jp301857m>.
- 873 (34) Djamali, E.; Tomson, M. B.; Chapman, W. G. Thermodynamic Properties and Solubility  
874 of Sodium and Potassium Chloride in Ethane-1,2-Diol/Water Mixed Solvent Systems to

- 875 High Temperatures. *J. Chem. Eng. Data* **2017**, 62 (4), 1326–1334.  
876 <https://doi.org/10.1021/acs.jced.6b00842>.
- 877 (35) Hála, E. Vapor-Liquid Equilibria of Strong Electrolytes in Systems Containing Mixed  
878 Solvent. *Fluid Phase Equilib.* **1983**, 13, 311–319.  
879 [https://doi.org/https://doi.org/10.1016/0378-3812\(83\)80102-2](https://doi.org/https://doi.org/10.1016/0378-3812(83)80102-2).
- 880 (36) Iliuta, M. C.; Thomsen, K.; Rasmussen, P. Extended UNIQUAC Model for Correlation  
881 and Prediction of Vapour-Liquid-Solid Equilibria in Aqueous Salt Systems Containing  
882 Non-Electrolytes. Part A. Methanol-Water-Salt Systems. *Chem. Eng. Sci.* **2000**, 55 (14),  
883 2673–2686. [https://doi.org/10.1016/S0009-2509\(99\)00534-5](https://doi.org/10.1016/S0009-2509(99)00534-5).
- 884 (37) Thomsen, K.; Iliuta, M. C.; Rasmussen, P. Extended UNIQUAC Model for Correlation  
885 and Prediction of Vapor-Liquid-Liquid-Solid Equilibria in Aqueous Salt Systems  
886 Containing Non-Electrolytes. Part B. Alcohol (Ethanol, Propanols, Butanols)-Water-Salt  
887 Systems. *Chem. Eng. Sci.* **2004**, 59 (17), 3631–3647.  
888 <https://doi.org/10.1016/j.ces.2004.05.024>.
- 889 (38) Fosbøl, P. L.; Thomsen, K.; Stenby, E. H. Modeling of the Mixed Solvent Electrolyte  
890 System CO<sub>2</sub>-Na<sub>2</sub>CO<sub>3</sub>-NaHCO<sub>3</sub>-Monoethylene Glycol-Water. *Ind. Eng. Chem. Res.*  
891 **2009**, 48 (9), 4565–4578. <https://doi.org/10.1021/ie801168e>.
- 892 (39) Guggenheim, E. A. L. The Specific Thermodynamic Properties of Aqueous Solutions of  
893 Strong Electrolytes. *London, Edinburgh, Dublin Philos. Mag. J. Sci.* **1935**, 19 (127), 588–  
894 643. <https://doi.org/10.1080/14786443508561403>.
- 895 (40) Christensen, C.; Sander, B.; Fredenslund, A.; Rasmussen, P. Towards the Extension of  
896 UNIFAC to Mixtures with Electrolytes. *Fluid Phase Equilib.* **1983**, 13 (C), 297–309.  
897 [https://doi.org/10.1016/0378-3812\(83\)80101-0](https://doi.org/10.1016/0378-3812(83)80101-0).
- 898 (41) Pitzer, K. S. *Activity Coefficients in Electrolyte Solutions*, 2nd Editio.; CRC Press: Boca  
899 Raton Ann Arbor Boston London, 1991.
- 900 (42) Robinson, R. A.; Sinclair, D. A. The Activity Coefficients of the Alkali Chlorides and of  
901 Lithium Iodide in Aqueous Solution from Vapor Pressure Measurements. *J. Am. Chem.*  
902 *Soc.* **1934**, 56 (9), 1830–1835. <https://doi.org/10.1021/ja01324a003>.
- 903 (43) Robinson, R. A. The Osmotic and Activity Coefficient Data of Some Aqueous Salt  
904 Solutions from Vapor Pressure Measurements. *J. Am. Chem. Soc.* **1937**, 59 (1), 84–90.  
905 <https://doi.org/10.1021/ja01280a019>.

- 906 (44) Robinson, R. A. The Activity Coefficients of Some Alkali Halides at 25.°. *Trans. Faraday*  
907 *Soc.* **1939**, *35*, 1217–1220.
- 908 (45) Mussini, P. R.; Mussini, T.; Sala, B. Thermodynamics of the Cell {Li-Amalgam | LiX (m)  
909 | AgX | Ag} (X = Cl,Br) and Medium Effects upon LiX in (Acetonitrile + Water), (1,4-  
910 Dioxane + Water), and (Methanol + Water) Solvent Mixtures with Related Solvation  
911 Parameters. *J. Chem. Thermodyn.* **2000**, *32* (5), 597–616.  
912 <https://doi.org/10.1006/jcht.1999.0622>.
- 913 (46) Yang, R.; Demirgian, J.; Solsky, J. F.; Kikta, E. J.; Marinsky, J. A. Mean Molal Activity of  
914 Sodium Chloride, Potassium Chloride, and Cesium Chloride in Ethanol-Water Mixtures. *J.*  
915 *Phys. Chem.* **1979**, *83* (21), 2752–2761. <https://doi.org/10.1021/j100484a013>.
- 916 (47) Westhaus, U. DETHERM. DECHEMA e.V.: Frankfurt am Main 2019.
- 917 (48) Thomsen, K. Data Bank for Electrolyte Solutions. Technical University of Denmark: Kgs.  
918 Lyngby 2020.
- 919 (49) Advanced Tools for Optimization and Uncertainty Treatment. IFP Energies nouvelles:  
920 Rueil-Malmaison 2019.
- 921 (50) Span, R.; Wagner, W. A New Equation of State for Carbon Dioxide Covering the Fluid  
922 Region from the Triple-Point Temperature to 1100 K at Pressures up to 800 MPa. *J. Phys.*  
923 *Chem. Ref. Data* **1996**, *25* (6), 1509–1596. <https://doi.org/10.1063/1.555991>.
- 924 (51) Chen, C.; Britt, H. I.; Boston, J. F.; Evans, L. B. Local Composition Model for Excess  
925 Gibbs Energy of Electrolyte Systems. Part I: Single Solvent, Single Completely  
926 Dissociated Electrolyte Systems. *AIChE J.* **1982**, *28* (4), 588–596.
- 927 (52) Chen, C. -C; Evans, L. B. A Local Composition Model for the Excess Gibbs Energy of  
928 Aqueous Electrolyte Systems. *AIChE J.* **1986**, *32* (3), 444–454.  
929 <https://doi.org/10.1002/aic.690320311>.
- 930 (53) Chen, C. C. Toward Development of Activity Coefficient Models for Process and Product  
931 Design of Complex Chemical Systems. *Fluid Phase Equilib.* **2006**, *241* (1–2), 103–112.  
932 <https://doi.org/10.1016/j.fluid.2006.01.006>.
- 933 (54) Saravi, S. H.; Ravichandran, A.; Khare, R.; Chen, C. C. Bridging Two-Liquid Theory with  
934 Molecular Simulations for Electrolytes: An Investigation of Aqueous NaCl Solution.  
935 *AIChE J.* **2019**, *65* (4), 1315–1324. <https://doi.org/10.1002/aic.16521>.
- 936 (55) Renon, H.; Prausnitz, J. M. Local Compositions in Thermodynamic Excess Functions for

- 937 Liquid Mixtures. *AIChE J.* **1968**, *14* (1), 135–144. <https://doi.org/10.1002/aic.690140124>.
- 938 (56) Pitzer, K. S. Electrolytes. From Dilute Solutions to Fused Salts. *J. Am. Chem. Soc.* **1980**,  
939 *102* (9), 2902–2906. <https://doi.org/10.1021/ja00529a006>.
- 940 (57) Liu, Y.; Watanasiri, S. Representation of Liquid-Liquid Equilibrium of Mixed-Solvent  
941 Electrolyte Systems Using the Extended Electrolyte NRTL Model. *Fluid Phase Equilib.*  
942 **1996**, *116* (1–2), 193–200. [https://doi.org/10.1016/0378-3812\(95\)02887-0](https://doi.org/10.1016/0378-3812(95)02887-0).
- 943 (58) Robinson, R. A.; Stokes, R. H. *Electrolyte Solutions, 2nd Edition*; Dover Publications:  
944 Mineola, 2002.
- 945 (59) Rashin, A. A.; Honig, B. Reevaluation of the Born Model of Ion Hydration. *J. Phys.*  
946 *Chem.* **1985**, *89* (26), 5588–5593. <https://doi.org/10.1021/j100272a006>.
- 947 (60) Chang, C. K.; Lin, S. T. Extended Pitzer-Debye-Hückel Model for Long-Range  
948 Interactions in Ionic Liquids. *J. Chem. Eng. Data* **2020**, *65* (3), 1019–1027.  
949 <https://doi.org/10.1021/acs.jced.9b00368>.
- 950 (61) Song, Y.; Chen, C. C. Symmetric Electrolyte Nonrandom Two-Liquid Activity Coefficient  
951 Model. *Ind. Eng. Chem. Res.* **2009**, *48* (16), 7788–7797.  
952 <https://doi.org/10.1021/ie9004578>.
- 953 (62) Tsanas, C.; de Hemptinne, J.-C.; Mougin, P. Calculation of Phase and Chemical  
954 Equilibrium for Multiple Ion-Containing Phases Including Stability Analysis. *Chem. Eng.*  
955 *Sci.* **2021**, 117174. <https://doi.org/10.1016/j.ces.2021.117174>.
- 956 (63) Mohr, P. J.; Newell, D. B.; Taylor, B. N. CODATA Recommended Values of the  
957 Fundamental Physical Constants: 2014. *J. Phys. Chem. Ref. Data* **2016**, *45*, 043102.  
958 <https://doi.org/10.1063/1.4954402>.
- 959 (64) Wilding, W. V.; Rowley, R. L.; Oscarson, J. L. DIPPR® Project 801 Evaluated Process  
960 Design Data. *Fluid Phase Equilib.* **1998**, *150* (151), 413–420.  
961 [https://doi.org/10.1016/s0378-3812\(98\)00341-0](https://doi.org/10.1016/s0378-3812(98)00341-0).
- 962 (65) Raspo, I.; Neau, E. An Empirical Correlation for the Relative Permittivity of Liquids in a  
963 Wide Temperature Range: Application to the Modeling of Electrolyte Systems with a  
964 GE/EoS Approach. *Fluid Phase Equilib.* **2020**, *506*, 112371.  
965 <https://doi.org/10.1016/j.fluid.2019.112371>.
- 966 (66) Xu, Y.; Li, S.; Zhai, Q.; Jiang, Y.; Hu, M. Investigation on the Thermodynamic Properties  
967 of KCl/CsCl + NaCl + CH<sub>3</sub>OH + H<sub>2</sub>O Quaternary Systems at 298.15K. *J. Ind. Eng.*



- 968 *Chem.* **2014**, *20* (4), 2159–2165. <https://doi.org/10.1016/j.jiec.2013.09.046>.
- 969 (67) Basili, A.; Mussini, P. R.; Mussini, T.; Rondinini, S. Thermodynamics of the Cell:  
970 {Na<sub>x</sub>Hg<sub>1-x</sub>|NaCl(m)|AgCl|Ag} in (Methanol + Water) Solvent Mixtures. *J. Chem.*  
971 *Thermodyn.* **1996**, *28* (8), 923–933. <https://doi.org/10.1006/jcht.1996.0081>.
- 972 (68) Yang, S. O.; Lee, C. S. Vapor-Liquid Equilibria of Water + Methanol in the Presence of  
973 Mixed Salts. *J. Chem. Eng. Data* **1998**, *43* (4), 558–561.  
974 <https://doi.org/10.1021/je970286w>.
- 975 (69) Basili, A.; Mussini, P. R.; Mussini, T.; Rondinini, S.; Vertova, A. Thermodynamics of the  
976 Amalgam Cell: {Me<sub>x</sub>Hg<sub>1-x</sub>|MeCl(m)|AgCl|Ag} (with Me = K, Rb) in (Methanol+water)  
977 Solvent Mixtures. *Berichte der Bunsengesellschaft für Phys. Chemie* **1997**, *101* (5), 842–  
978 846. <https://doi.org/https://doi.org/10.1002/bbpc.19971010510>.
- 979 (70) Estes, M. A.; Gonzalez-Diaz, O. M.; Hernandez-Luis, F. F.; Fernandez-Merida, L.  
980 Activity Coefficients for NaCl in Ethanol-Water Mixtures at 25 C. *J. Solution Chem.* **1989**,  
981 *18* (3), 277–288.
- 982 (71) Mamontov, M. N.; Konstantinova, N. M.; Uspenskaya, I. A. Water-Ethanol-Sodium  
983 Chloride System: The Main Sources of Uncertainties in Thermodynamic Properties  
984 Determined by Potentiometry. *Fluid Phase Equilib.* **2016**, *412*, 62–70.  
985 <https://doi.org/10.1016/j.fluid.2015.12.012>.
- 986 (72) Mussini, P. R.; Mussini, T.; Perelli, A.; Rondinini, S.; Vertova, A. Thermodynamics of the  
987 Cell: {Me<sub>x</sub>Hg<sub>1-x</sub>|MeCl(m)|AgCl|Ag} (Me = Na, K, Cs) in (Ethanol + Water) Solvent  
988 Mixtures. *J. Chem. Thermodyn.* **1995**, *27* (3), 245–251.  
989 <https://doi.org/https://doi.org/10.1006/jcht.1995.0022>.
- 990 (73) Yan, Y.; Chen, C. C. Thermodynamic Representation of the NaCl+Na<sub>2</sub>SO<sub>4</sub>+H<sub>2</sub>O System  
991 with Electrolyte NRTL Model. *Fluid Phase Equilib.* **2011**, *306* (2), 149–161.  
992 <https://doi.org/10.1016/j.fluid.2011.03.023>.
- 993 (74) Harned, H. S. A Rule for the Calculation of the Activity Coefficients of Salts in Organic  
994 Solvent-Water Mixtures. *J. Phys. Chem.* **1962**, *66* (4), 589–591.  
995 <https://doi.org/10.1021/j100810a004>.
- 996 (75) Basili, A.; Mussini, P. R.; Mussini, T.; Rondinini, S.; Sala, B.; Vertova, A. Transference  
997 Numbers of Alkali Chlorides and Characterization of Salt Bridges for Use in  
998 Methanol+water Mixed Solvents. *J. Chem. Eng. Data* **1999**, *44* (5), 1002–1008.

- 999 <https://doi.org/10.1021/je9900979>.
- 1000 (76) Hu, M.; Tang, J.; Li, S.; Xia, S.; Jiang, Y. Activity Coefficients of Lithium Chloride in  
1001 ROH/Water Mixed Solvent (R = Me, Et) Using the Electromotive Force Method at 298.15  
1002 K. *J. Chem. Eng. Data* **2008**, *53* (2), 508–512. <https://doi.org/10.1021/je700614h>.
- 1003 (77) Broul, M.; Hlavatý, K.; Linek, J. Liquid-Vapour Equilibrium in Systems of Electrolytic  
1004 Components. V. The System CH<sub>3</sub>OH-H<sub>2</sub>O-LiCl at 60 °C. *Collect. Czechoslov. Chem.*  
1005 *Commun.* **1969**, *34* (11), 3428–3435.
- 1006 (78) Yao, J.; Yan, W. D.; Xu, Y. J.; Han, S. J. Activity Coefficients for NaCl in MeOH + H<sub>2</sub>O  
1007 by Electromotive Force Measurements at 308.15 K and 318.15 K. *J. Chem. Eng. Data*  
1008 **1999**, *44* (3), 497–500. <https://doi.org/10.1021/je970288g>.
- 1009 (79) Hernández-Hernández, F.; Pérez-Villaseñor, F.; Hernández-Ruiz, V.; Iglesias-Silva, G. A.  
1010 Activity Coefficients of NaCl in H<sub>2</sub>O + MeOH + EtOH by Electromotive Force at 298.15  
1011 K. *J. Chem. Eng. Data* **2007**, *52* (3), 959–964. <https://doi.org/10.1021/je600549h>.
- 1012 (80) Yao, J.; Li, H.; Han, S. Vapor-Liquid Equilibrium Data for Methanol-Water-NaCl at  
1013 45 °C. *Fluid Phase Equilib.* **1999**, *162* (1–2), 253–260. [https://doi.org/10.1016/S0378-](https://doi.org/10.1016/S0378-3812(99)00204-6)  
1014 [3812\(99\)00204-6](https://doi.org/10.1016/S0378-3812(99)00204-6).
- 1015 (81) Johnson, A. I.; Furter, W. F. Salt Effect in Vapor-Liquid Equilibrium. *Can. J. Chem. Eng.*  
1016 **1960**, *38* (3), 78–87.
- 1017 (82) Zhang, J.; Gao, S.-Y.; Xia, S.-P.; Yao, Y. Study of Thermodynamic Properties of  
1018 Quaternary Mixture RbCl + Rb<sub>2</sub>SO<sub>4</sub> + CH<sub>3</sub>OH + H<sub>2</sub>O by EMF Measurement at 298.15  
1019 K. *Fluid Phase Equilib.* **2004**, *226* (1–2), 307–312.  
1020 <https://doi.org/10.1016/j.fluid.2004.10.010>.
- 1021 (83) Hu, M.; Cui, R.; Li, S.; Jiang, Y.; Xia, S. P. Determination of Activity Coefficients for  
1022 Cesium Chloride in Methanol-Water and Ethanol-Water Mixed Solvents by Electromotive  
1023 Force Measurements at 298.15 K. *J. Chem. Eng. Data* **2007**, *52* (2), 357–362.  
1024 <https://doi.org/10.1021/je060278s>.
- 1025 (84) Cui, R. F.; Hu, M. C.; Jin, L. H.; Li, S. N.; Jiang, Y. C.; Xia, S. P. Activity Coefficients of  
1026 Rubidium Chloride and Cesium Chloride in Methanol-Water Mixtures and a Comparative  
1027 Study of Pitzer and Pitzer-Simonson-Clegg Models (298.15 K). *Fluid Phase Equilib.* **2007**,  
1028 *251* (2), 137–144. <https://doi.org/10.1016/j.fluid.2006.11.016>.
- 1029 (85) Falciola, L.; Longoni, G.; Mussini, P. R.; Mussini, T. Thermodynamics of the Amalgam

- 1030 Cells {Cs-Amalgam|CsX (m)|AgX|Ag} (X = Cl, Br, I) and Primary Medium Effects in  
1031 (Methanol + Water), (Acetonitrile + Water), and (1,4-Dioxane + Water) Solvent Mixtures.  
1032 *J. Chem. Thermodyn.* **2006**, *38* (6), 788–798. <https://doi.org/10.1016/j.jct.2005.08.014>.
- 1033 (86) Hernández-Luis, F.; Vázquez, M. V; Estesó, M. A. Activity Coefficients for NaF in  
1034 Methanol-Water and Ethanol-Water Mixtures at 25 °C. *J. Mol. Liq.* **2003**, *108* (1), 283–  
1035 301. [https://doi.org/https://doi.org/10.1016/S0167-7322\(03\)00187-9](https://doi.org/https://doi.org/10.1016/S0167-7322(03)00187-9).
- 1036 (87) BOONE, J. E.; ROUSSEAU, R. W.; SCHOENBORN, E. M. The Correlation of Vapor-  
1037 Liquid Equilibrium Data for Salt-Containing Systems. In *Thermodynamic Behavior of*  
1038 *Electrolytes in Mixed Solvents*; Advances in Chemistry; AMERICAN CHEMICAL  
1039 SOCIETY, 1976; Vol. 155, pp 36–52. <https://doi.org/doi:10.1021/ba-1976-0155.ch004>.
- 1040 (88) Han, S.; Pan, H. Thermodynamics of the Sodium Bromide-Methanol-Water and Sodium  
1041 Bromide-Ethanol-Water Two Ternary Systems by the Measurements of Electromotive  
1042 Force at 298.15K. *Fluid Phase Equilib.* **1993**, *83* (C), 261–270.  
1043 [https://doi.org/10.1016/0378-3812\(93\)87029-Z](https://doi.org/10.1016/0378-3812(93)87029-Z).
- 1044 (89) Hernández-Luis, F.; Galleguillos, H. R.; Graber, T. A.; Taboada, M. E. Activity  
1045 Coefficients of LiCl in Ethanol - Water Mixtures at 298.15 K. *Ind. Eng. Chem. Res.* **2008**,  
1046 *47* (6), 2056–2062. <https://doi.org/10.1021/ie070704i>.
- 1047 (90) Shaw, R.; Butler, J. A. V. The Behavior of Electrolytes in Mixed Solvents. Part II. - The  
1048 Effect of Lithium Chloride on the Activities of Water and Alcohol in Mixed Solvents.  
1049 *Proc. R. Soc. London. Ser. A - Math. Phys. Sci.* **1930**, *129*, 519–536.
- 1050 (91) Meyer, T.; Poika, H. M.; Gmehling, J. Low-Pressure Isobaric Vapor-Liquid Equilibria of  
1051 Ethanol/Water Mixtures Containing Electrolytes. *J. Chem. Eng. Data* **1991**, *36* (3), 340–  
1052 342. <https://doi.org/10.1021/je00003a023>.
- 1053 (92) Sun, R. Molecular Thermodynamics of Salt Effect in Vapor-Liquid Equilibrium -  
1054 Calculation of Isobaric VLE Salt Effect Parameters for Ethanol-Water-1-1 Type  
1055 Electrolyte Systems. *CIESC J.* **1996**, *47* (4), 401-409 (in Chinese).
- 1056 (93) González-Díaz, O. M.; Fernández-Mérida, L.; Hernández-Luis, F.; Estesó, M. A. Activity  
1057 Coefficients for NaBr in Ethanol-Water Mixtures at 25 °C. *J. Solution Chem.* **1995**, *24* (6),  
1058 551–563. <https://doi.org/10.1007/BF00973206>.
- 1059 (94) BURNS, J. A.; FURTER, W. F. Effects of Salts Having Large Organic Ions on Vapor-  
1060 Liquid Equilibrium. In *Advances in Chemistry, Thermodynamic Behavior of Electrolytes*

- 1061 *in Mixed Solvents*; Advances in Chemistry; AMERICAN CHEMICAL SOCIETY, 1976;  
1062 Vol. 155, pp 99–127. <https://doi.org/doi:10.1021/ba-1976-0155.ch008>.
- 1063 (95) Du, Y.; Tang, J.; Li, S.; Zhai, Q.; Jiang, Y.; Hu, M. Activity Coefficients for CsBr +  
1064 MeOH/EtOH + H<sub>2</sub>O Ternary Systems Using Potentiometric Measurements at 298.15 K. *J.*  
1065 *Chem. Eng. Data* **2012**, 57 (9), 2603–2609. <https://doi.org/10.1021/je300671y>.
- 1066 (96) Yamamoto, H.; Terano, T.; Yanagisawa, M.; Tokunaga, J.; Nishi, Y.; Tokunaga, J. Salt  
1067 Effect of CaCl<sub>2</sub>, NH<sub>4</sub>i and NaI on Vapor-Liquid Equilibrium of Ethanol + Water  
1068 System at 298.15 K. *Can. J. Chem. Eng.* **1995**, 73 (5), 779–783.  
1069 <https://doi.org/https://doi.org/10.1002/cjce.5450730522>.
- 1070 (97) Burns, J. A.; Furter, W. F. Salt Effect in Vapor-Liquid Equilibrium At Fixed Liquid  
1071 Composition. *Adv. Chem. Ser.* **1979**, No. 177, 11–26. [https://doi.org/10.1021/ba-1979-](https://doi.org/10.1021/ba-1979-0177.ch002)  
1072 [0177.ch002](https://doi.org/10.1021/ba-1979-0177.ch002).
- 1073 (98) Akerlof, G. Activity Coefficients of Sodium, Potassium and Lithium Chlorides and  
1074 Hydrochloric Acid at Infinite Dilution in Water-Methyl Alcohol Mixtures. *J. Am. Chem.*  
1075 *Soc.* **1930**, 52, 2353–2368.
- 1076 (99) Yan, W.; Xu, Y.; Han, S. Activity Coefficients of Sodium Chloride in Methanol-Water  
1077 Mixed Solvents at 298.15 K. *Acta Chim. Sin.* **1994**, 52 (10), 937-946 (in Chinese).
- 1078 (100) Deyhimi, F.; Abedi, M. NaCl + CH<sub>3</sub>OH + H<sub>2</sub>O Mixture: Investigation Using the Pitzer  
1079 and the Modified Pitzer Approaches to Describe the Binary and Ternary Ion-  
1080 Nonelectrolyte Interactions. *J. Chem. Eng. Data* **2012**, 57 (2), 324–329.  
1081 <https://doi.org/10.1021/je201084a>.
- 1082 (101) Kozłowski, Z.; Bald, A.; Gregorowicz, J. Thermodynamic Studies of NaCl Solutions in  
1083 Water + Methanol Mixtures by Means of a Galvanic Cell Containing a Glass Sodium  
1084 Electrode. *J. Electroanal. Chem.* **1990**, 288 (1–2), 75–82. [https://doi.org/10.1016/0022-](https://doi.org/10.1016/0022-0728(90)80026-3)  
1085 [0728\(90\)80026-3](https://doi.org/10.1016/0022-0728(90)80026-3).
- 1086 (102) Jödecke, M.; Kamps, Á. P. S.; Maurer, G. Experimental Investigation of the Influence of  
1087 NaCl on the Vapor-Liquid Equilibrium of CH<sub>3</sub>OH + H<sub>2</sub>O. *J. Chem. Eng. Data* **2005**, 50  
1088 (1), 138–141. <https://doi.org/10.1021/je049783k>.
- 1089 (103) Sun, R. Calculation of Salting Effect on Vapor-Liquid Equilibrium in Water-  
1090 Nonelectrolyte Systems. *Chem. Eng.* **1995**, 23 (1), 13–17, 30 (in Chinese).
- 1091 (104) Abedi, M.; Shendi, M. A.; Karimzadeh, Z.; Salamat-Ahangari, R.; Deyhimi, F. The

1092 Ternary and Quaternary Electrolyte Systems: Activity Coefficient of NaCl Measured and  
1093 Modeled for NaCl + C<sub>2</sub>H<sub>5</sub>OH + H<sub>2</sub>O and NaCl + KCl + C<sub>2</sub>H<sub>5</sub>OH + H<sub>2</sub>O Systems. *Fluid*  
1094 *Phase Equilib.* **2016**, *423*, 138–145. <https://doi.org/10.1016/j.fluid.2016.04.023>.  
1095 (105) Chen, W.; Zhang, W. Vapor-Liquid Equilibria for Alcohol-Water-KI/NaAc Systems. *J.*  
1096 *Chem. Eng. Chinese Univ.* **2003**, *17* (2), 123-127 (in Chinese).  
1097